# Recent progress in alkaline water electrolysis for hydrogen production and applications

Kai Zeng [1], Dongke Zhang[*]

Centre for Petroleum, Fuels and Energy (M050), The School of Mechanical Engineering, The University of Western Australia, 35 Stirling Highway, Crawley, WA 6009, Australia

## ARTICLE INFO

## ABSTRACT

Alkaline water electrolysis is one of the easiest methods for hydrogen production, offering the advantage of simplicity. The challenges for widespread use of water electrolysis are to reduce energy consumption, cost and maintenance and to increase reliability, durability and safety. This literature review examines the current state of knowledge and technology of hydrogen production by water electrolysis and identifies areas where R&D effort is needed in order to improve this technology. Following an overview of the fundamentals of alkaline water electrolysis, an electrical circuit analogy of resistances in the electrolysis system is introduced. The resistances are classified into three categories, namely the electrical resistances, the reaction resistances and the transport resistances. This is followed by a thorough analysis of each of the resistances, by means of thermodynamics and kinetics, to provide a scientific guidance to minimising the resistance in order to achieve a greater efficiency of alkaline water electrolysis. The thermodynamic analysis defines various electrolysis efficiencies based on theoretical energy input and cell voltage, respectively. These efficiencies are then employed to compare different electrolysis cell designs and to identify the means to overcome the key resistances for efficiency improvement. The kinetic analysis reveals the dependence of reaction resistances on the alkaline concentration, ion transfer, and reaction sites on the electrode surface, the latter is determined by the electrode materials. A quantitative relationship between the cell voltage components and current density is established, which links all the resistances and manifests the importance of reaction resistances and bubble resistances. The important effect of gas bubbles formed on the electrode surface and the need to minimise the ion transport resistance are highlighted. The historical development and continuous improvement in the alkaline water electrolysis technology are examined and different water electrolysis technologies are systematically compared using a set of the practical parameters derived from the thermodynamic and kinetic analyses. In addition to the efficiency improvements, the needs for reduction in equipment and maintenance costs, and improvement in reliability and durability are also established. The future research needs are also discussed from the aspects of electrode materials, electrolyte additives and bubble management, serving as a comprehensive guide for continuous development of the water electrolysis technology.

© 2009 Elsevier Ltd. All rights reserved.

## Contents

* Corresponding author. Tel.: +61 8 6488 8668.
  E-mail addresses: kzeng@mech.uwa.edu.au (K. Zeng), dongke.zhang@uwa.edu.au (D. Zhang).
[1] Tel.: +61 8 6488 3782.

## 1. Introduction

Hydrogen is mainly used in petroleum refining [1,2], ammonia production [3,4] and, to a lesser extent, metal refining such as nickel, tungsten, molybdenum, copper, zinc, uranium and lead [5,6], amounts to more than 50 million metric tonnes worldwide in 2006 [7]. The large scale nature of such hydrogen consumptions requires large scale hydrogen production to match them. As such, the hydrogen production is dominated by reforming of natural gas [8] and gasification of coal and petroleum coke [9,10], as well as gasification and reforming of heavy oil [11,12]. Although water electrolysis to produce hydrogen (and oxygen) has been known for around 200 years [13,14] and has the advantage of producing extremely pure hydrogen, its applications are often limited to small scale and unique situations where access to large scale hydrogen production plants is not possible or economical, such as marine, rockets, spacecrafts, electronic industry and food industry as well as medical applications. Water electrolysis represents only 4% of the world hydrogen production [15,16].

With ever increasing energy costs owing to the dwindling availability of oil reserves, production and supply [17] and concerns with global warming and climate change blamed on man-made carbon dioxide ($CO_2$) emissions associated with fossil fuel use [18], particularly coal use [2], hydrogen has in recent years become very popular for a number of reasons: (1) it is perceived as a clean fuel, emits almost nothing other than water at the point of use; (2) it can be produced using any energy sources, with renewable energy being most attractive [19]; (3) it works with fuel cells [20–22] and together, they may serve as one of the solutions to the sustainable energy supply and use puzzle in the long run, in so-called "hydrogen economy" [23,24].

Water electrolysis can work beautifully well at small scales and, by using renewable electricity, it can also be considered more sustainable. In a conceptual distributed energy production, conversion, storage and use system for remote communities, as illustrated in Fig. 1, water electrolysis may play an important role in this system as it produces hydrogen using renewable energy as a fuel gas for heating applications and as an energy storage

mechanism. When abundant renewable energy is available, excessive energy may be stored in the form of hydrogen by water electrolysis. The stored hydrogen can then be used in fuel cells to generate electricity or used as a fuel gas. A number of studies have been reported according to the different renewable energy sources. Isherwood et al. [25] presented an analytical optimisation of a remote system for a hypothetical Alaskan village. In this paper, wind and solar energies are utilised to reduce the usage of diesel for electricity generation. The electricity generated by the renewable energy is either merged into the grid or used to produce hydrogen or zinc. With such a hybrid energy system, 50% of diesel fuel and 30% annual cost savings by wind turbines were estimated. Energy storage devices such as phosphoric acid fuel cell and zinc-air fuel cell were found to be helpful to reduce the fuel consumption
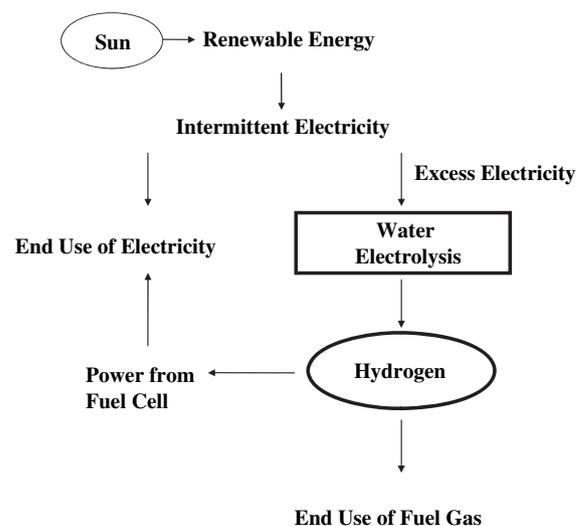


**Fig. 1.** A schematic illustration of a conceptual distributed energy system with water electrolysis playing an important role in hydrogen production as a fuel gas and energy storage mechanism.

**Nomenclature**

| | |
|---|---|
| $A$ | surface area of electrode or cross-section area of conductance ($cm^2$ or $m^2$) |
| $A$ | frequency factor (dimensionless) |
| $C$ | concentration or coulomb (electrical charge) ($mol\,m^{-3}$ or C) |
| $E$ | electrode potential or energy (V or (J or kJ)) |
| $E_A$ | activation energy (kJ) |
| $F$ | Faraday's constant ($96{,}485\,C\,mol^{-1}$) |
| $f$ | volume fraction ratio (dimensionless) |
| $G$ | Gibbs free energy (J) |
| $H$ | enthalpy (J) |
| $i$ or $I$ | current (A) |
| $i_0$ | exchange current density ($A\,m^{-2}$) |
| $j$ | current density ($A\,m^{-2}$) |
| $k$ | reaction rate constant ($mol\,L^{-1}\,s^{-1}$) |
| $K$ | Kohlrausch coefficient (dimensionless) |
| $K_{sp}$ | solubility constant (dimensionless) |
| $l$ or $L$ | length (m) |
| $n$ | number of electrons transferred (dimensionless) |
| $N$ | the number of one species (dimensionless) |

| | |
|---|---|
| $O$ | oxidation production of $R$ (dimensionless) |
| $Q$ | electrical charge (C) |
| $r$ | production rate ($m^3\,h^{-1}$) |
| $R$ | electrical resistance, gas constant or reduction production of O ($\Omega$, $8314\,J\,K^{-1}\,mol^{-1}$ or dimensionless) |
| $t$ | time (s) |
| $T$ | temperature (°C or K) |
| $U$ | electrical voltage (V) |
| $V$ | volume or unit of the voltage ($m^3$ or V) |
| $x$ | distance (m) |
| $\alpha$ | transit coefficient (dimensionless) |
| $\gamma$ | surface tension (N) |
| $\eta$ | efficiency (dimensionless) |
| $\eta$ | overpotential (mV) |
| $\theta$ | gas surface coverage or contact angle (dimensionless or ° (degree)) |
| $\kappa$ | electrical conductivity ($\Omega^{-1}\,m^{-1}$) |
| $\rho$ | resistivity of gas solution mixture ($\Omega\,m$) |
| $\Lambda$ | molar conductivity of an electrolyte ($\Omega^{-1}\,m^2\,mol^{-1}$) |
| $\Delta$ | difference operator |
| $\sum$ | summation operator |
| ° | standard |

further. Young et al. [26] considered the technical and economic feasibility of using renewable energy with hydrogen as the energy storage mechanism for remote community in the mountain area of Sengor, Bhutan. The abundant hydro power, at $840\,MWh\,year^{-1}$, can not only satisfy the need of local lighting and other household uses, but can also be exported to India. Electrolyser capable of producing hydrogen at the rate of $20\,Nm^3\,h^{-1}$ is proposed. The practical problems of extending the grid over long distance and mountainous terrain could then be solved by using such a system. Hanley and Nevin [27] applied two economic appraisal techniques to evaluate three renewable energy options for a remote community in North West Scotland. Economic benefits, environmental implications and tourism are taken into account. The authors believe that the renewable energy development may well be beneficial for remote rural communities. Although Hanley et al.'s work does not include hydrogen, we believe that if the renewable energy options referred to in their study are coupled with hydrogen production and use, it will provide much greater flexibility and reliability of the systems.

Remote areas with abundant solar and/or wind electricity resources can take advantage of the water electrolysis to produce hydrogen to meet their energy need for households such as lighting and heating [28], powering telecommunication stations [29] and small-scale light manufacturing industry applications, electricity peak shaving, and in integrated systems, both grid-connected and grid-independent [30]. Hydrogen produced by renewable energy has a great advantage, mobility, which is essential to the energy supply in remote areas away from the main electricity grid. Agbossou et al. [31] studied an integrated renewable energy system for powering remote communication stations. The system is based on the production of hydrogen by water electrolysis whereby electricity is generated by a 10 kW wind turbine and a 1 kW photovoltaic array. When power is needed the electricity is regenerated from the stored hydrogen via a 5 kW proton exchange membrane (PEM) fuel cell system. The system gives stable electrical power for communication stations. Degiorgis et al. [32] studied the feasibility of a hydrogen fuelled trial village which was based on hydrogen as the primary fuel. In this work, the hydrogen is produced by water electrolysis and stored for the use in hydrogen vehicles and for thermal purposes (heating requirement of three buildings). Water electrolysers are

designed to produce $244{,}440\,N\,m^3\,year^{-1}$ of $H_2$, with an energy efficiency of 61%. The light industry applications of water electrolysis may include mechanical workshops where hydrogen and oxygen gases produced from water electrolysis can replace oxygen–acetylene for metal braising, cutting and welding [33,34].

Small-scale water electrolysers can avoid the need for a large fleet of cryogenic, liquid hydrogen tankers or a massive hydrogen pipeline system. The existing electrical power grid could be used as the backbone of the hydrogen infrastructure system, contributing to the load levelling by changing operational current density in accordance with the change in electricity demand [35]. A small-scale pure hydrogen and oxygen can find diverse applications including gases in laboratories and oxygen to life-support system in hospitals [36].

While possessing these advantages of availability, flexibility and high purity, to achieve widespread applications, hydrogen production using water electrolysis needs improvements in energy efficiency, safety, durability, operability and portability and, above all, reduction in costs of installation and operation. These open up many new opportunities for research and development leading to technological advancements in water electrolysis. This literature review aims to identify such new research and development opportunities. We begin with an overview of the fundamentals of water electrolysis in the context of electrochemistry, laying a theoretical basis for scientific analysis of the published electrolysis systems and data. We then analyse various water electrolysis techniques in a broad range of applications and examine recent trends in research and innovations to identify the gaps for improvements – the needs for further research and development.

## 2. Electrolysis fundamentals

### 2.1. Chemistry of water electrolysis

A basic water electrolysis unit consists of an anode, a cathode, power supply, and an electrolyte, as illustrated in Fig. 2. A direct current (DC) is applied to maintain the electricity balance and electrons flow from the negative terminal of the DC source to the cathode at which the electrons are consumed by hydrogen ions (protons) to form hydrogen. In keeping the electrical charge (and valence) in balance, hydroxide ions (anions) transfer through the
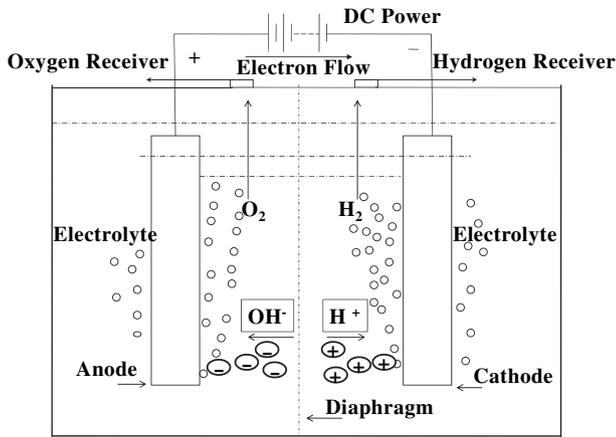
**Fig. 2.** A schematic illustration of a basic water electrolysis system.

electrolyte solution to anode, at which the hydroxide ions give away electrons and these electrons return to the positive terminal of the DC source. In order to enhance the conductivity of the solution, electrolytes which generally consist of ions with high mobility are applied in the electrolyser [37]. Potassium hydroxide is most commonly used in water electrolysis, avoiding the huge corrosion loss caused by acid electrolytes [38]. Nickel is a popular electrode material due to its high activity and availability as well as low cost [39]. However, the introduction of these conductive components could also bring about some side effects, which will be discussed in the following sections. During the process of water electrolysis, hydrogen ions move towards cathode, and hydroxide ions, move towards the anode. By the use of a diaphragm, gas receivers can collect hydrogen and oxygen, which form on and depart from the cathode and the anode, respectively.

The half reactions occurring on the cathode and anode, respectively, can be written as

$$\text{Cathode}: \quad 2H^+ + 2e \rightarrow H_2 \tag{R1}$$

$$\text{Anode}: \quad 2OH^- \rightarrow \frac{1}{2}O_2 + H_2O + 2e \tag{R2}$$
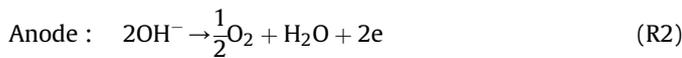
The overall chemical reaction of the water electrolysis can be written as

$$H_2O \rightarrow H_2 + \frac{1}{2}O_2 \tag{R3}$$

### 2.2. Electrical circuit analogy of water electrolysis cells

For this electrochemical reaction process to proceed, a number of barriers have to be overcome, requiring a sufficient electrical energy supply. These barriers include electrical resistance of the circuit, activation energies of the electrochemical reactions occurring on the surfaces of the electrodes, availability of electrode surfaces due to partial coverage by gas bubbles formed and the

resistances to the ionic transfer within the electrolyte solution. It is important that these barriers are analysed in the contexts of thermodynamics and kinetics as well as transport process principles.

Fig. 3 shows the resistances (the barriers) presented in a typical water electrolysis system. The first resistance from the left-hand-side $R_1$ is the external electrical circuit resistance including the wiring and connections at anode. $R_{\text{anode}}$ is originated from the overpotential of the oxygen evolution reaction on the surface of the anode. $R_{\text{bubble,O}_2}$ is the resistance due to partial coverage of the anode by the oxygen bubbles, hindering the contact between the anode and the electrolyte. The resistances come from electrolyte and membrane are noted as $R_{\text{ions}}$ and $R_{\text{membrane}}$, respectively. Similarly, $R_{\text{bubble,H}_2}$ roots from the blockage of the cathode by hydrogen bubbles; $R_{\text{cathode}}$ is the resistance caused by the over-potential for oxygen evolution reaction and $R_1'$ is the electrical resistance of the wiring and connections at cathode. Thus, the total resistance can be expressed in Equation (1).

$$R_{\text{Total}} = R_1 + R_{\text{anode}} + R_{\text{bubble,O}_2} + R_{\text{ions}} + R_{\text{membrane}} + R_{\text{bubble,H}_2} \\ + R_{\text{cathode}} + R_1' \tag{1}$$

These resistances in electrolysis systems can be classified into three categories, the first category includes all the electrical resistances; the second includes the reaction resistances; and the third includes the transport resistances.

#### 2.2.1. Electrical resistances

The *electrical* resistances can be calculated using the Ohm's law: $R = U/I$ [37], in which $I$ is the current when voltage $U$ is applied only at the circuit. Or, it can be calculated from the physics equation: $R = L/(\kappa A)$, in which $L$, $\kappa$ and $A$ are the length, specific conductivity and cross-sectional area of the conductor, respectively. $R_1$ and $R_1'$ belong to this category and are usually considered as one integral part $R_{\text{cir}}$.

#### 2.2.2. Transport-related resistances

These are the *physical* resistances experienced in the electrolysis process such as gas bubbles covering the electrode surfaces and present in the electrolyte solution, resistances to the ionic transfer in the electrolyte and due to the membrane used for separating the $H_2$ and $O_2$ gases. $R_{\text{bubble,O}_2}$, $R_{\text{ions}}$, $R_{\text{membrane}}$ and $R_{\text{bubble,H}_2}$ are considered as transport resistances.

Both electrical resistances and transport resistances cause heat generation according to the Joule's law [37] and transport phenomena [40] and thus inefficiency of the electrolysis system. The lost energy due to these resistances is also known as the ohmic loss [41].

#### 2.2.3. Electrochemical reaction resistances

The *reaction resistances* are due to the overpotentials required to overcome the activation energies of the hydrogen and oxygen formation reactions on the cathode and anode surfaces, which directly cause the increase in the overall cell potential. These are the inherent energy barriers of the reactions, determining the kinetics of the electrochemical reactions [42].
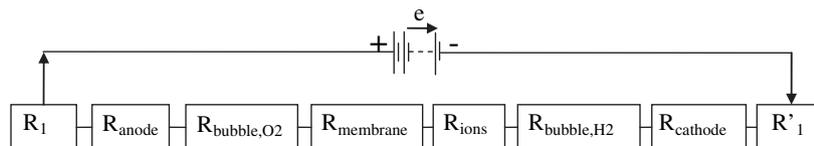


**Fig. 3.** An electrical circuit analogy of resistances in the water electrolysis system.

The reaction resistances or overpotentials are inherent resistances of the electrochemical reactions depending on the surface activities of the electrodes employed. $R_{anode}$ and $R_{cathode}$ are reaction resistances.

Clearly, the strategies in any effort to improve the energy efficiency of water electrolysis and thus the performance of the system must involve the understanding of these resistances so as to minimise them.

## 3. Thermodynamic consideration

### 3.1. Theoretical cell voltages

Water is one of the thermodynamically most stable substances in the nature and it is always an uphill battle to try to pull water molecules apart to make its elements into hydrogen and oxygen molecules. No pain, no gain. If we want hydrogen (and oxygen) from water by electrolysis, we have to at least overcome an *equilibrium cell voltage*, $E°$, which is also called "electromotive force". With established reversibility and absence of cell current between the two different electrode reactions, the open cell potential is called the equilibrium cell voltage, it is defined as equilibrium potential difference between the respective anode and cathode [43] and is described by Equation (2).

$$E° = E°_{anode} - E°_{cathode} \qquad (2)$$

Equation (3) relates the change in the Gibbs free energy $\Delta G$ of the electrochemical reaction to the equilibrium cell voltage as follows.

$$\Delta G = nFE° \qquad (3)$$

where $n$ is the number of moles of electrons transferred in the reaction, and $F$ is the Faraday constant. The overall water electrolysis cell reaction, $E°$ (25 °C) is 1.23 V and the Gibbs free energy change of the reaction is $+237.2$ kJ mol$^{-1}$ [44], which is the minimum amount of electrical energy required to produce hydrogen. The cell voltage at this point is known as *reversible potential*. Hence the electrolysis of water to hydrogen and oxygen is thermodynamically unfavourable at room temperature and can only occur when sufficient electrical energy is supplied. In contrast, when the electrolysis process is performed under adiabatic conditions, the total reaction enthalpy must be provided by electrical current. Under this circumstance, the *thermo-neutral* voltage is required to maintain the electrochemical reaction without heat generation or adsorption [45].

Therefore, even when the equilibrium potential is met, the electrode reactions are inherently slow and then an *overpotential* $\eta$, above the equilibrium cell voltage is necessary in order to kick start the reaction due to the activation energy barrier, low reaction rate and the bubble formation [42,46]. According to the resistances mentioned above, input of additional energy is also essential to drive the ionic migration process and overcome the resistance of the membrane as well as the electrical circuit. This extra energy requirement causes a *potential drop*, $iR_{cell}$, (where $i$ is the current through the cell and $R_{cell}$ is the sum of electrical resistance of the cell, a function of electrolyte properties, the form of the electrodes and cell design) within the cell. The *cell potential* $E_{cell}$ can be written as Equation (4), which is always 1.8–2.0 V at the current density of 1000–300 A m$^{-2}$ in industry water electrolysis [47]. The total overpotential is the sum of overpotentials or barriers from the hydrogen and oxygen evolution reactions, electrolyte concentration difference and bubble formation. If one has a mild condition under which gas bubble and concentration differences can be neglected, the sum of overpotential can be calculated using

Equation (5), where $j$ is the current density (current divided by electrode surface area) at which electrolysis cell operates. Both of the overpotential and the ohmic loss increase with current density and may be regarded as causes of inefficiencies in the electrolysis whereby electrical energy is degraded into heat which must be taken into account in any consideration of energy balance.

$$E_{cell} = E_{anode} - E_{cathode} + \sum \eta + iR_{cell} \qquad (4)$$

$$\sum \eta = |\eta_{anode}(j)| + |\eta_{cathode}(j)| \qquad (5)$$

Fig. 4 shows the relationship between the electrolyser cell potential and operating temperature [17,48]. The cell potential–temperature plane is divided into three zones by the so-called equilibrium voltage line and thermo-neutral voltage line. The equilibrium voltage is the theoretical minimum potential required to dissociate water by electrolysis, below which the electrolysis of water cannot proceed. The equilibrium voltage deceases with increasing temperature. The thermo-neutral voltage is the actual minimum voltage that has to be applied to the electrolysis cell, below which the electrolysis is endothermic and above which, exothermic. The thermo-neutral voltage naturally includes the overpotentials of the electrodes, which are only weakly dependent on temperature. Thus, the thermo-neutral voltage only exhibits a slight increase with temperature. We denote thermo-neutral voltage as $E_{\Delta H}$. If water electrolysis takes place in the shaded area in Fig. 4, the reaction will be endothermic.

### 3.2. Cell efficiencies

Energy efficiency is commonly defined as the percentage share of the energy output in the total energy input. However, there are a number of ways of expressing the efficiency of electrolysis, depending on how the electrolysis system is assessed and compared.

Generally, in the electrochemistry sense, the *voltage efficiency* of an electrolysis cell can always be calculated using Equation (6) [17,49].

$$\%\text{voltage efficiency} = \frac{(E_{anode} - E_{cathode})100}{E_{cell}} \qquad (6)$$

The physical meaning of this equation is the proportion of effective voltage to split water in the total voltage applied to the whole
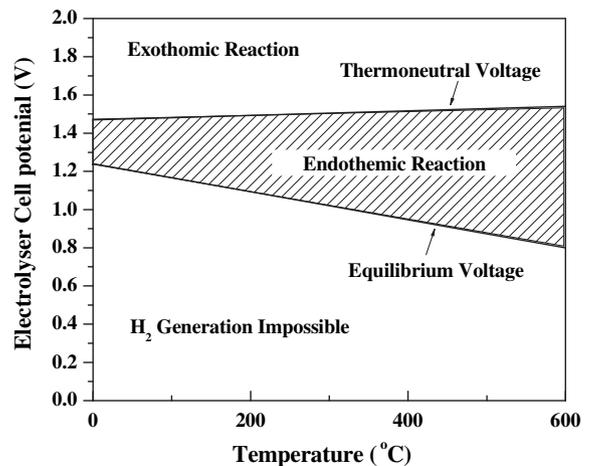


**Fig. 4.** Cell potential for hydrogen production by water electrolysis as a function of temperature.

electrolysis cell. It is a good approximation of the efficiency of the electrolysis system.

There are two other efficiencies calculated based on the energy changes of the water electrolysis reaction, known as the *Faradic efficiency* and the *thermal efficiency*. They use the Gibbs free energy change and enthalpy change of water decomposition reaction as the energy input, respectively. Both $\eta_{\text{Faradic}}$ and $\eta_{\text{Thermal}}$ adopt the theoretical energy requirement plus energy losses as the energy input. As shown in Equations (7) and (8).

$$\eta_{\text{Faradic}} = \frac{\Delta G}{\Delta G + \text{Losses}} = \frac{E_{\Delta G}}{E_{\text{cell}}} \tag{7}$$

$$\eta_{\text{Thermal}} = \frac{\Delta H}{\Delta G + \text{Losses}} = \frac{E_{\Delta H}}{E_{\text{cell}}} \tag{8}$$

Both equations can be simplified using cell potential and total cell voltage as shown in Equations (9) and (10)

$$\eta_{\text{Faradic}} (25^{\circ}\text{C}) = \frac{1.23 \ (\text{V})}{E_{\text{cell}}} \tag{9}$$

$$\eta_{\text{Thermal}} (25^{\circ}\text{C}) = \frac{1.48 \ (\text{V})}{E_{\text{cell}}} \tag{10}$$

where the $E_{\text{cell}}$ is cell voltage. $E_{\Delta G}$ and $E_{\Delta H}$ are the equilibrium and thermo-neutral voltages, respectively.

The physical meaning of Equation (7) is the percentage of the theoretical energy needed to force apart the water molecules in the real cell voltage and is a measure of the cell efficiency purely from the cell voltage point of view. On the contrast, Equation (8) means that an additional cell voltage, above the reversible voltage, is required to maintain the thermal balance and the percentage of the actual energy input in the real voltage defines the thermal efficiency. It is then possible that the thermal efficiency of a water electrolysis cell may exceed 100% as the system may absorb heat from the ambient if it operates in endothermic mode (in the shaded area of Fig. 4).

The Gibbs free energy and the enthalpy of the reaction are also a function of temperature as illustrated in Fig. 4. Equations (9) and (10) give the efficiencies at 25 °C. The values of Faradic efficiency are always less than 1 because there are always losses. While the thermal efficiency can be higher than 1 provided the water electrolysis operates under a voltage lower than the thermo-neutral voltage. This phenomenon is due to that heat is absorbed from the environment. When the denominator in Equation (8) is 1.48 V, the electrolysis operates at the efficiency of 100%. No heat will be absorbed from or released to the environment.

In practice, if the potential drop caused by electrical resistance is 0.25 V and 0.6 V for the cathode and anode overpotentials at 25 °C, respectively, the Faradic efficiency is $(1.23 * 100\%)/(1.23 + 0.25 + 0.6) = 59\%$, and the thermal efficiency is $(1.48 * 100\%)/(1.23 + 0.25 + 0.6) = 71\%$. The electrolysis cell is exothermic at cell potential above 1.48 V, and endothermic at cell potential below this value. The Faradic efficiency investigates the electrolysis reaction while the thermal efficiency takes the whole thermal balance into account.

Yet another means to compare and evaluate the efficacy of a water electrolysis systems is to consider the output of hydrogen production against the total electrical energy applied to the system, in both terms of hydrogen production rate and energy (the high heating value of hydrogen) carried by the hydrogen produced.

$$\eta_{\text{H}_2 \text{production rate}} = \frac{r_{\text{H}_2 \text{production rate}}}{\Delta E} = \frac{V \left( \text{m}^3 \text{m}^{-3} \text{h}^{-1} \right)}{Uit \ (\text{kJ})} \tag{11}$$

where the $U$ is the cell voltage, $i$ is the current, $t$ stands for time. $V$ is the hydrogen production rate at unit volume electrolysis cell. The physical meaning of Equation (11) is the hydrogen production rate per unit electrical energy input. It is a way for direct comparison of hydrogen production capacity of different electrolysis cells, or

$$\eta_{\text{H}_2 \text{yield}} = \frac{E_{\text{Useable}}}{\Delta E} = \frac{283.8 \ (\text{kJ})}{Uit} \tag{12}$$

where 283.8 kJ is the high heating value (HHV) of one mole hydrogen and $t$ is for the time needed for one gram hydrogen produced.

An alternative expression of the energy efficiency is to subtract the energy losses from the total energy input as shown in Equation (13).

$$\eta_{\text{net efficiency}} = 1 - \frac{E_{\text{loss}}}{E_{\text{input}}} \tag{13}$$

where $E_{\text{loss}}$ can be expressed in terms of the resistances discussed in Equation (1). Those resistances cause respective energy losses. By considering these resistances an analogous electrical unit, each of them can be calculated using the Joule's Law. Therefore,

$$\begin{aligned} E_{\text{loss}} = \sum E_{\text{loss},i} &= E_{\text{loss,circuit}} + E_{\text{loss,anode}} + E_{\text{loss,O}_2\text{bubble}} \\ &+ E_{\text{loss,ion}} + E_{\text{loss,membrane}} + E_{\text{loss,anode}} + E_{\text{loss,H}_2\text{bubble}} \end{aligned} \tag{14}$$

Equation (14) identifies all the components of energy losses, which can then be rated, allowing the efficiency to be improved by targeting the key causes of energy loss components.

From the discussion above, we can conclude that there are two broad ways of energy efficiency improvement: one is to thermodynamically reduce the energy needed to split water to yield hydrogen, such as by increasing the operating temperature or pressure; the other is to reduce the energy losses in the electrolysis cell, which can be realised by minimising the dominant components of the resistances.

In addition to the thermodynamic analysis of water electrolysis, various system parameters such as electrode materials, electrolyte properties and reaction temperatures can affect the performance of electrochemical cells. It is necessary to discuss the kinetics of the electrode reactions.

## 4. Electrode kinetics

The rate of the electrode reaction, characterised by the current density, firstly depends on the nature and pre-treatment of the electrode surfaces. Secondly, the rate of reaction depends on the composition of the electrolytic solution adjacent to the electrodes. These ions in the solution near the electrodes, under the effect of electrode, form layers, known as *double layer* [37], taking cathode for example, the charge layer formed by hydroxyl ions and potassium ions according to the charge of the electrodes. Finally, the rate of the reaction depends on the electrode potential, characterised by the reaction overpotential. The study of electrode kinetics seeks to establish the macroscopic relationship between the current density and the surface overpotential and the composition of the electrolytic solution adjacent to the electrode surface [50].

The double layer is illustrated in Fig. 5(a). The accumulated ions form two mobile layers of solvent molecules and adsorbed species. The one nearer the electrode surface is relatively ordered, termed the inner Helmholtz layer (IHL). The other one with less order is called outer Helmholtz layer (OHL) [51]. The electrical charges on the surface of the electrodes are balanced by ionic counter-charges in the vicinity of the electrodes. The potential distribution is also plotted against the distance from the electrode surface in Fig. 5(b).
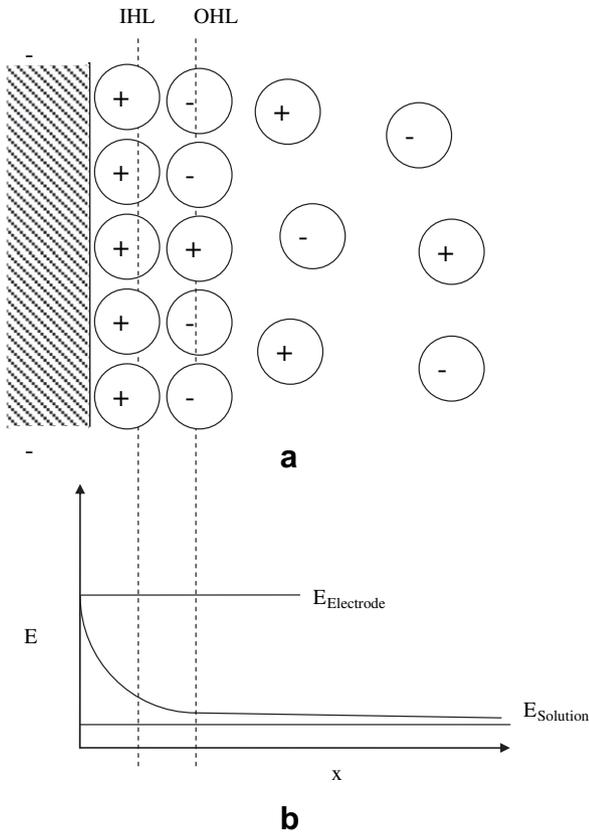
**Fig. 5.** A schematic illustration of electrical double layer and the potential distribution near an electrode surface.

It can be clearly seen that the interfacial potential difference exists between the electrode surface and the solution due to the existence of the double layer [43].

The phenomenon of the double layer formation is a non-faradic process [43]. It leads to the capacitive behaviour of the electrode reactions. This capacitor property of electrode surfaces should be taken into consideration in the kinetics.

According to the Faraday's law, the number of moles of the electrolysed species ($H^+$ or $O^{2-}$), $N$, is given by

$$N = \frac{Q}{nF} \tag{15}$$

where $Q$ is the total charge in Coulomb transferred during the reaction, $n$ is the stoichiometric number of electrons consumed in the electrode reaction ($n = 2$ for both reactions R1 and R2), $F$ is the Faraday constant. The rate of electrolysis can be expressed as

$$\text{Rate} = \frac{dN}{dt} \tag{16}$$

$dQ/dt$ can be noted as Faradic current $i$ [42].

Generally the surface area at which the reaction takes place needs to be taken into account. The rate of the electrolysis reaction can be expressed as

$$\text{Rate} = \frac{i}{nFA} = \frac{j}{nF} \tag{17}$$

where $j$ is the current density.

The rate constant of a chemical reaction can be in general expressed by the Arrhenius equation.

$$k = Ae^{\frac{E_A}{RT}} \tag{18}$$

where, $E_A$ stands for the *activation energy*, kJ mol$^{-1}$, A is the *frequency factor*. $R$ is the gas constant, and $T$ is reaction temperature. Although the equation is oversimplified, it reveals the relationship between the activation energy and the rate constant.

For one-step, one-electron reaction, through the relationship between the current and the reaction rate, the dependence of the current density on the surface potential and the composition of the electrolytic solution adjacent to the electrode surface is given by the Butler–Volmer equation [42]:

$$i = i_{\text{cath}} - i_{\text{anode}}$$
$$= FAk^0 \left( C_O(0,t)e^{-\alpha f(E-E^\circ)} - C_R(0,t)e^{f(1-\alpha)(E-E^\circ)} \right) \tag{19}$$

where $A$ is the electrode surface area through which the current passes, $k^0$ is the *standard rate constant*, $\alpha$ refers to the *transfer coefficient* its value lies between 0 and 1 for this one-electron reaction, $f$ is the $F/RT$ ratio. $t$ and 0 in the bracket are, respectively, the specific time at which this current occurs and the distance from the electrode. For the half reaction R1, $C_O(0,t)$ stands for the concentration of reaction species at cathode in the oxided state, the hydrogen ions ($H^+$), while $C_R(0,t)$ is the concentration of reaction product hydrogen $(1/2)H_2$, which is in the reduced state.

Equation (19) is derived using the transition-state-theory [42]. The theory describes a set of curvilinear coordinates in the reaction path as shown in Fig. 6(a). The potential energy is a function of the independent positions of the coordinates in the system. When a potential increases by $\Delta E$, it will cause the relative energy of the electron to decrease by $F(E - E^\circ)$ as illustrated in Fig. 6(a). The decrease in turn reduces the Gibbs free energy of the hydrogen ions in the hydrogen evolution reaction by $(1 - \alpha)(E - E^\circ)$ and, on the contrast, increases the Gibbs free energy of hydrogen by $\alpha(E - E^\circ)$, respectively. Therefore, provided that there is no mass transfer limitation, the Butler–Volmer equation can be derived from Equations (17) and (18) using the Gibbs free energy changes in Fig. 6.
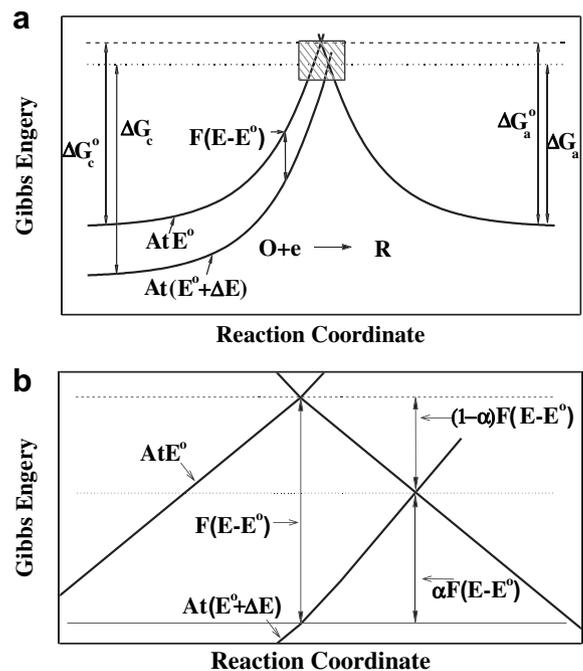


**Fig. 6.** Effect of potential change on Gibbs energy energies: (a) the overall relationship between energy change and state of reaction and (b) magnified picture of shaded area of (a).

The Butler–Volmer equation can be simplified as:

$$i = i_0\left(e^{-\alpha f\eta} - e^{(1-\alpha)f\eta}\right) \tag{20}$$

where $i_0$ is known as the exchange current density [52], which is the current of the reversible water splitting reaction. From the simplified equation above, we can derive the overpotential at each electrode, respectively. In the absence of the influence of mass transfer and at the large overpotentials ($>$118 mV at 25°), one of the terms in equation (14) can be neglected. For example, at large negative overpotential, $e^{-\alpha f\eta} \gg e^{(1-\alpha)f\eta}$. the relationship between $i$ and $\eta(E - E^\circ)$ can be written in the Tafel equation [53]:

$$\eta = a + b \log i \tag{21}$$

where $a = (2.3RT)/(\alpha F)\log i_0$ and $b = (-2.3RT)/(\alpha F)$.

The linear relationship between the overpotential and the logarithm of current density is characterised by the slope $b$ and exchange current density $i_0$. The slope is also known as Tafel slope. Both parameters are commonly used as kinetic data to compare electrodes in electrochemistry.

From the above analysis, the rate of the electrolysis can be expressed by the current or current density. Furthermore the current can be reflected by $i_0$, which is the current associated with the reversible reaction on the surface of the electrodes. The rate of the reaction is also directly determined by the overpotential, which depends on a number of factors. One of the important factors is the activation energy, $E_A$, which is strongly influenced by the electrode material, thus a focus of continuing research effort. To reduce the activation energies of the electrode reactions, or reduce the overpotential, it is therefore necessary to consider how they are related to the electrode materials and surface configurations.

### 4.1. Hydrogen generation overpotential

The mechanism of the hydrogen evolution reaction is widely accepted [17] to be a step involving the formation of adsorbed hydrogen

$$H^+ + e^- \rightarrow H_{ads} \tag{R4}$$

which is followed by either chemical desorption

$$2H_{ads} \rightarrow H_2 \tag{R5}$$

or electrochemical desorption

$$H^+ + e^- + H_{ads} \rightarrow H_2 \tag{R6}$$

where the subscript ads represents the adsorbed status.

The overpotential of hydrogen is generally measured by the Tafel equation

$$\eta_{cathode} = 2.3\frac{RT}{\alpha F}\log\frac{i}{i_0} \tag{22}$$

In this equation, $i_0$, the exchange current density of the reaction, which can be analogised as the rate constant of reaction, is a function of the nature of the electrode (cathode) material [50]. The overpotential of the hydrogen production means extra energy barrier in the process of hydrogen formation.

The overpotential on the cathode is directly related to the formation of hydrogen in the vicinity of the electrode. The formation of hydrogen is intrinsically determined by the bond between hydrogen and the electrode surface. Pd has the lowest heat of adsorption of hydrogen ($83.5\ kJ\ mol^{-1}$) as compared to $105\ kJ\ mol^{-1}$ for Ni [54]. Meanwhile, the hydrogen formation is also influenced by

the electrode properties, the type and concentration of electrolyte and temperature. By comparing the kinetic data including the exchange current density and Tafel slope, the relationship between these factors can be revealed. Table 1 compares the kinetic parameters, represented by the current density and Tafel slope, of the hydrogen evolution reactions on different metal electrode materials.

For hydrogen evolution reaction, it is necessary to identify the rate determining step. If the hydrogen adsorption, R4, is the rate determining step, electrode material with more edges and cavities in its surface structure which favour easy electron transfer will create more electrolysis centres for hydrogen adsorption. If the hydrogen desorptions, R5 and R6, are the rate determining step, physical properties such as surface roughness or perforation will either increase the electron transfer by adding reaction area or preventing the bubbles from growing, which in turn increase the rate of electrolysis.

Increasing the overpotential could lead to a mechanism change. In other words, the rate determining step will alter within different potential ranges. When the potential is low, the electron transfer is not as fast as desorption. The hydrogen adsorption will be the rate determining step. On the contrast, when the potential is high enough to enable the hydrogen adsorption rate to be greater than the desorption rate, the hydrogen desorption will be the rate determining step.

### 4.2. Oxygen generation overpotential

The mechanism of oxygen evolution reaction is more complex compared to the pathways suggested for the hydrogen evolution reaction. There are a number of theories presented and discussed in the literature and the most generally accepted mechanism involves the following steps:

$$OH_{ads}^- \rightleftharpoons OH_{ads} + e^- \tag{R7}$$

$$OH^- + OH_{ads}^- \rightleftharpoons O_{ads} + H_2O + e^- \tag{R8}$$

$$O_{ads} + O_{ads} \rightleftharpoons O_2 \tag{R9}$$

One of the charge transfer steps is rate controlling. The dependence of transfer coefficients $\alpha$ in Equation (19) and Tafel slope variations can be used to identify the rate determining step. For example, a slow electron transfer step (R7) determines the reaction at low temperatures, on the contrast, a slow recombination step (R9) controls at high temperatures on nickel electrode. The different Tafel slopes between the steps can be used to judge the mechanisms [51,59].

The overpotential of oxygen evolution reaction is generally measured by the Tafel equation

$$\eta_{anode} = 2.3\frac{RT}{(1-\alpha)F}\log\frac{i}{i_0} \tag{23}$$

**Table 1**
Kinetics parameters of hydrogen production on different electrode metals.

| Metal | Heat of $H_2$ adsorption ($kJ\ mol^{-1}$) | Electrolyte | Temperature (°C) | $i_0$ ($A\ m^{-2}$) | Tafel slope (mV) |
|---|---|---|---|---|---|
| Ni [55] | 105 | 1 M NaOH | 20 | $1.1 \times 10^{-2}$ | 121 |
| Fe [56] | 109 | 2 M NaOH | 20 | $9.1 \times 10^{-2}$ | 133 |
| Pb [57] | N/A | 6 N NaOH | 25 | $4 \times 10^{-2}$ | 121 |
| Zn [57] | N/A | 6 N NaOH | 25 | $8.5 \times 10^{-6}$ | 124 |
| Co [58] | N/A | 0.5 M NaOH | 25 | $4.0 \times 10^{-3}$ | 118 |
| Pt [17] | 101 | 0.1 N NaOH | 22 | 4.0 | 105 |
| Au [17] | N/A | 0.1 N NaOH | 25 | $4.0 \times 10^{-2}$ | 120 |

The reaction rate decreases with increasing activation energy, so reducing the activation energy is always favoured for more efficient water electrolysis. Furthermore, the activation energy increases with increasing current density and can be lowered by using appropriate electrocatalysts. Table 2 compares the kinetic parameters, again represented by the current density and Tafel slope, of oxygen evolution reactions on different metal electrode materials.

Generally speaking, the overpotential of oxygen evolution is more difficult to reduce than that of hydrogen evolution, owing to the complex mechanism and irreversibility. Alloys of Fe and Ni have been found to be able to reduce the overpotential to some extent [63].

### 4.3. Cell overpotential

As shown above, the hydrogen and oxygen overpotentials can be expressed by Equations (22) and (23). A typical plot in Fig. 7 is the Tafel plot as a function of Equation (21) in water electrolysis. The parameters used to compare the electrode kinetics are the exchange current $i_0$ and the Tafel slope. A higher exchange current density and lower slope indicate a higher electrode activity.

Since the cell potential contains both anode and cathode reactions, identifying the contributions of each of anode and cathode to the cell voltage and factors influencing them is necessary to understand the overpotential resistance. The typical effect of temperature on the overpotential is summarised by Kinoshita [47]. As shown in Fig. 8 an increase in temperature will result in a decrease in the overpotential at the same current density.

The overpotential is not only a function of temperature but also a function of current density [38]. As can be seen from Fig. 9, the overpotentials from hydrogen and oxygen evolutions are the main sources of the reaction resistances. The other obvious resistance at high current densities is the Ohmic loss in the electrolyte, which includes resistances from the bubbles, diaphragm and ionic transfer. Understanding these resistances opens up opportunities to enhance the efficiency of the water electrolysis.

## 5. Electrical and transport resistances

### 5.1. Electrical resistances

The electrical resistances are the direct reasons of heat generation which leads to the wastage of electrical energy in the form of heat formation according to the Ohms law. The electrical resistances in a water electrolysis system have three main components: (1) the resistances in the system circuits; (2) The mass transport phenomena including ions transfer in the electrolyte; (3) The gas bubbles covering the electrode surfaces and the diaphragm.

The resistances of electrodes and connection circuits are determined by the types and dimensions of the materials, preparation methods, and the conductivities of the individual components. It can be expressed as follows:

$$R = \sum \frac{l}{A\kappa_g} \tag{24}$$

**Table 2**
Kinetic parameters of oxygen production on different metals.

| Metal | Electrolyte | Temperature (°C) | $i_0$ (A m$^{-2}$) | Tafel slope (mV) |
|---|---|---|---|---|
| Pt [60] | 30% KOH | 80 | $1.2 \times 10^{-5}$ | 46 |
| Ir [61] | 1 N NaOH | N/A | $1.0 \times 10^{-7}$ | 40 |
| Rh [61] | 1 N NaOH | N/A | $6.0 \times 10^{-8}$ | 42 |
| Ni [62] | 50% KOH | 90 | $4.2 \times 10^{-2}$ | 95 |
| Co [60] | 30% KOH | 80 | $3.3 \times 10^{-2}$ | 126 |
| Fe [60] | 30% KOH | 80 | $1.7 \times 10^{-1}$ | 191 |
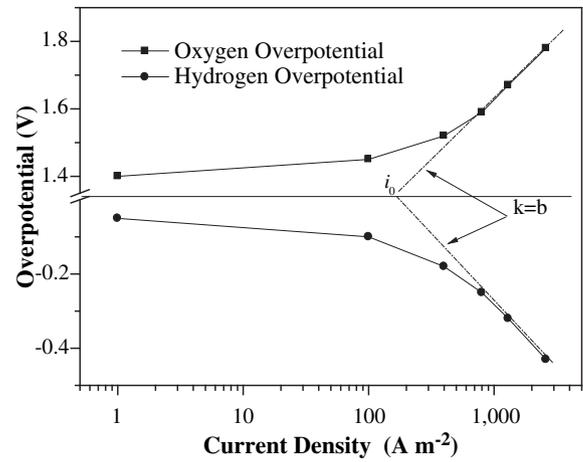


**Fig. 7.** Typical Tafel plots for both hydrogen and oxygen evolution.

where $\kappa$ is the electrical conductivity and has the unit of $\Omega^{-1}$ m$^{-1}$, subscript $g$ stands for each component of the circuit, including wires, connectors and the electrode. This part of the resistance can be reduced by reducing the length of the wire, increasing the cross-section area and adopting more conductive wire material.

Ionic transfer within the electrolyte depends on the electrolyte concentration and separation distance between the anodes and cathodes, the diaphragm between the electrodes. Different from the conductance rate in the metallic conductor, the *Molar conductivity* is adopted to replace the conductivity and can be expressed as follows:

$$\Lambda = \frac{\kappa}{C} \tag{25}$$

where $C$ is the electrolyte concentration. The unit of the molar conductivity is m$^2$ $\Omega^{-1}$ mol$^{-1}$. It is also a function of concentration and the mass transfer rate of the ions. As strong electrolytes are commonly applied in the water electrolysis, the empirical relationship between $\Lambda_C$ and $C$ is given in

$$\Lambda_C = \Lambda_0 - K\sqrt{C} \tag{26}$$

where $\Lambda_0$ is the mole conductivity extrapolated to infinite dilution which is known. $K$ is the Kohlrausch coefficient, a proportionality constant of the linear relationship between molar conductivity and square root of concentration [52]. In terms of ionic resistance, improvements can be made by increasing the conductivity of the
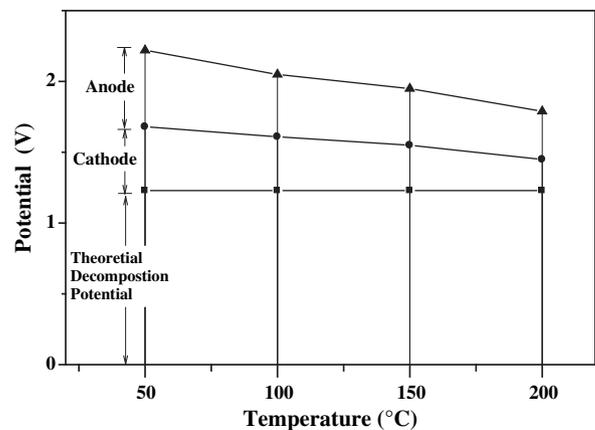


**Fig. 8.** An illustration of the contributions of anode and cathode polarisation to the cell voltage of an alkaline water electrolysis cell.
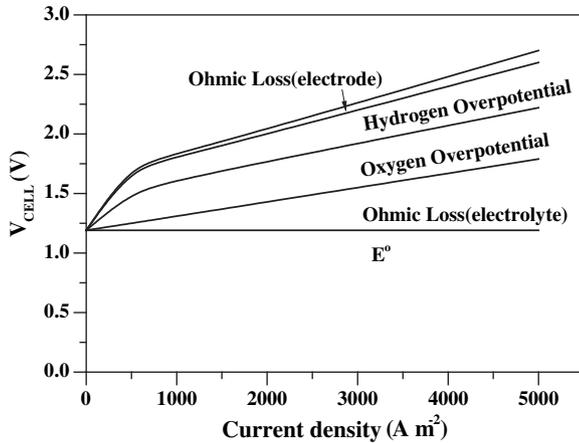
**Fig. 9.** Compositions of the typical cell voltage of an alkaline water electrolysis cell.

electrolyte by altering its concentration or adding appropriate additives.

The presence of bubbles in the electrolyte solution and on the electrode surfaces causes additional resistances to the ionic transfer and surface electrochemical reactions. One of the accepted theoretical equations to study the bubble effect in the electrolyte is given as follows [64]:

$$\kappa_g = \kappa(1 - 1.5f) \tag{27}$$

where $\kappa$ is the specific conductivity of the gas-free electrolyte solution; $f$ is the volume fraction of gas in the solution [51]. Quantitative illustration of the bubble resistance in terms of the bubble coverage on the surface and the bubble existence in the electrolytes needs to be considered. If we take bubble coverage into consideration, the bubble coverage is denoted as $\theta$, which represents the percentage of the electrode surface covered by the bubble. The electrical resistance caused by the bubble formation on the electrode surface can be calculated as follow [65],

$$\rho = \rho_0(1 - \theta)^{-\frac{3}{2}} \tag{28}$$

where $\rho_0$ is the specific resistivity of the gas-free electrolyte solution. If a diaphragm is used to separate the hydrogen and oxygen formed for collections, respectively, the presence of the diaphragm presents another resistance to the ionic transfer. The resistive effect associated with the diaphragm is expressed by MacMullin and Muccini [66] for the apparent conductivity:

$$\kappa_d = 0.272\frac{\kappa m^2}{p} \tag{29}$$

where $m$ is the hydraulic radius and $p$ is the permeability. The effective resistance of a membrane frequently amounts to between three and five times more than the resistance of the electrolyte solution of the same thickness as that of the membrane [51].

By dividing the overpotential by the current density, all of the resistances can be unified on the unit of ohm, which makes it possible to compare energy losses caused by different resistances as illustrated in Fig. 10, where, $E_{\text{loss, electrolyte}}$ includes energy losses due to the bubbles in the electrolyte and ionic transfer resistances. Fig. 10 also shows that the energy losses caused by the reaction resistances increase relatively slowly as the current density increases. The energy loss in the electrical circuit is relatively small. However, the energy loss due to the ionic transfer resistance in the electrolyte becomes more significant at higher current density. The dot and dash lines are the bubble resistance and total resistance. The energy loss due to bubble coverage on the electrode surfaces,

and thus the total energy loss are hypothetical, on the base of 50% electrode surface being covered by bubbles.

Although the relationship between the current density and energy loss in Fig. 10 does not specify all of the resistances mentioned before, it approximately presents the relationships among the losses. More interestingly, the energy loss due to bubbles formed on the electrodes should be considered as the major contribution to the total energy loss. Therefore, minimising the bubble effect holds a key to the electrolyser efficiency improvement.

### 5.2. Transport resistances

Convective mass transfer plays an important role in the ionic transfer, heat dissipation and distribution, and gas bubble behaviour in the electrolyte. The viscosity and flow field of the electrolyte determine the mass (ionic) transfer, temperature distribution and bubble sizes, bubble detachment and rising velocity, and in turn influence the current and potential distributions in the electrolysis cell. As the water electrolysis progresses the concentration of the electrolyte increases, resulting in an increase in the viscosity. Water is usually continuously added to the system to maintain a constant electrolyte concentration and thus the viscosity.

However, better mass transfer does not mean more hydrogen production. It is true that the mass transport leads to greater reaction rates, but the large number of gas bubbles formed, resulting from the increased reaction rate, can adversely hinder the contact between the electrodes and the electrolyte. The recirculation of electrolyte can be applied to mechanically accelerate the departure of the bubbles and bring them to the collectors.

The recirculation of the electrolyte is helpful in preventing the development of an additional overpotential due to the differences in electrolyte concentration in the cell. The velocity of fluid in the electrolyser can prompt the removal of the gas and vapour bubbles from the electrodes. On the other hand, the recirculation of the electrolyte can also help distribute the heat evenly within the electrolyte. At start-up, electrolyte circulation can be utilised to heat up the electrolyte to the operating temperature which is recommended to be 80–90 °C [47,67].

### 5.3. Bubble phenomena

As electrolysis progresses, hydrogen and oxygen gas bubbles are formed on the surfaces of the anode and cathode, respectively, and are only detached from the surface when they grow big enough. The coverage of the electrode surfaces by the gas bubbles directly
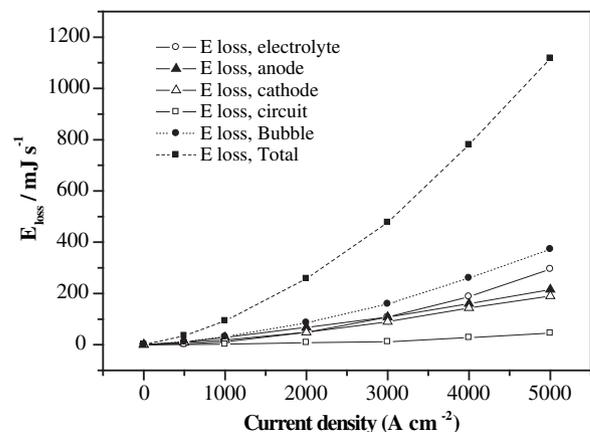


**Fig. 10.** A qualitative comparison of the energy losses caused by reaction resistances, ohmic resistance, ionic resistance and bubble resistance.

adds to the electrical resistance of the whole system, by reducing the contact between the electrolyte and the electrode, blocking the electron transfer, and increasing the ohmic loss of the whole system. Understanding the bubble phenomena is therefore an important element in the development of any water electrolysis systems. Mechanically circulating the electrolyte can accelerate the detachment of bubbles, providing a possible means to reduce the resistance due to gas bubbles. Alternatives are to consider the use of appropriate additives to the electrolyte solution to reduce the surface tension of the electrolyte and modifications of the electrode surface properties to make them less attractive to the gas bubbles.

Understanding the dynamics of the bubble behaviour is important in order to determine the conditions for the departure of the bubbles from the electrodes. The general thermodynamic condition for the three phase contact between the gas bubble, electrode and the electrolyte is a finite contact angle at the three phase boundary [68,69] as illustrated in Fig. 11.

The Young's equation defines the contact angle in terms of the three interfacial tensions [70],

$$\cos \theta = \frac{\gamma_{sv} - \gamma_{sl}}{\gamma_{lv}} \qquad (30)$$

where $\gamma_{sv}$, $\gamma_{lv}$ and $\gamma_{sl}$ are the surface tensions of the solid/vapour, solid/liquid and liquid/vapour interfaces, respectively. The Gibbs free energy change accompanying the replacement of the unit area of the solid/liquid interface by a solid/vapour interface

$$\Delta G = \gamma_{lv}(\cos \theta - 1) \qquad (31)$$

The detachment of the bubbles depends on the replacement of the electrolyte at the solid/solution interface, which is known as wettablity [71,72].

Two kinds of electrode surfaces can be defined according to the surface tension, namely, hydrophobic and hydrophilic. The electrode which favours water is hydrophilic, and the one does not is hydrophobic. Appropriate surface coating can therefore be applied to make the electrode surfaces more hydrophilic in order to reduce the surface coverage by the gas bubbles.

Therefore there are some broad approaches to manage the bubble phenomena. One is to treat the electrode surfaces to make them more hydrophilic so that water is more likely to take place of bubbles. Another is to use additives in the electrolyte solution to reduce surface tension so that bubbles are easy to depart from electrodes. In addition, controlling flow pattern to force bubbles to leave electrodes mechanically is also a means.

Intensive studies have been given to the bubble behaviour in the electrolysis systems [71,73–76]. It is a key issue to be resolved to overcome or reduce bubble resistance. Further detailed studies are necessary to further reduce the negative effects of the bubbles.
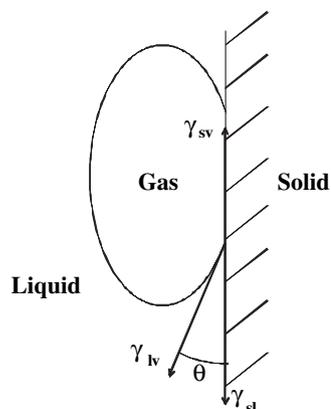
## 6. Practical considerations

In order to evaluate different electrolysis systems, it is necessary to relate a number of practical parameters to the performance of different electrolysers. The important parameters are categorised and discussed in the following discussion. These practical parameters for comparison of electrolysers include

- Cell configurations: bipolar and monopolar configurations, the gap between the electrodes as well as the flow velocity of the electrolytes.
- Operating conditions: including cell potential, current density, operating temperature and pressure, type and concentration of electrolytes as well as the stability of electrode material.
- External requirements: water quality requirement and system issues such as time space yield the quality of gases produced and safety issues.

### 6.1. Cell configurations

There are two alkaline electrolysis cell configurations, namely, the monopolar and the bipolar as shown in Fig. 12. In the monopolar arrangement, Fig. 12(a), alternate electrodes are directly connected to the opposite terminals of the DC power supply, respectively, giving a number of individual cells in parallel with one another. The total voltage applied to the whole electrolysis cell is essentially the same as that applied to the individual pairs of the electrodes in the cell. For the bipolar arrangement, Fig. 12(b), only two end electrodes are connected to the DC power supply. Thus every two adjacent electrodes form a unit cell, and these unit cells are electrically linked, via the electrolyse solution as the conducting



Fig. 11. An illustration of the contact angle at the three phase boundary of the gas bubble, electrode and the electrolyte.
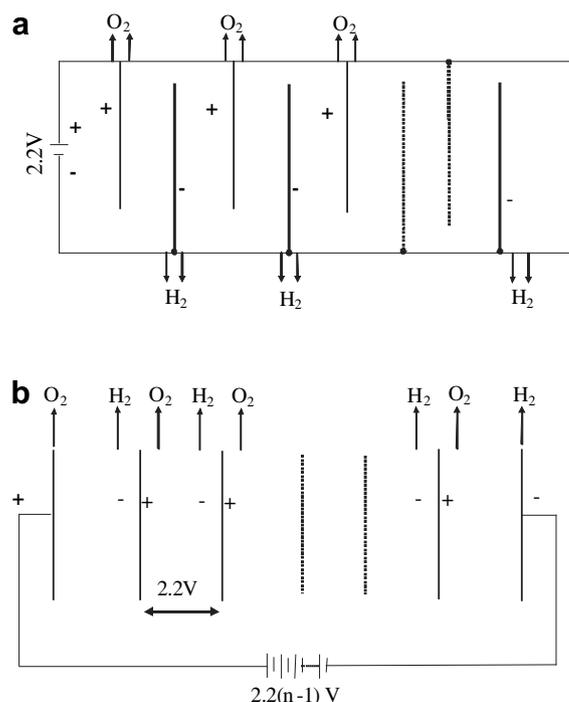


Fig. 12. Schematics of cell configurations of monopolar (a) and bipolar (b) electrolysers.

media, in series with one another. The total cell voltage is the sum of the individual unit cell voltages.

Due to the difference in the electrode arrangements, the reactions on the electrodes and the operation potentials are different for these two arrangements. In the monopolar configuration, the same electrochemical reaction, either the hydrogen evolution reaction or the oxygen evolution reaction, occurs on both sides of each electrode. However, in the bipolar configuration, the two different reactions evolving hydrogen and oxygen respectively, take place simultaneously on the opposite sides of the same electrodes that are not directly connected to the power source, that is, one side of an electrode acts as a cathode and the other as an anode (although both sides of the same electrode are at the same electric potential), except the two end electrodes that are connected to the DC power source. The cell operation potentials as the total voltage supplied by the DC power source are quite different for these two basic configurations; the typical value is normally 2.2 V for the monopolar configuration and $2.2 \times (n-1)$ V for the bipolar configuration (where $n$ is the number of electrodes) for industrial processes [17].

From the manufacturing point of view, the monopolar configuration is simple and easy to fabricate and maintain but suffers from high electrical currents at low voltages, causing large ohmic losses. The bipolar configuration reduces the ohmic losses on the electrical circuit connecters but demands much greater precision in design and manufacturing to prevent the electrolyte and gas leakage between cells [17].

Cell configurations also include the gaps between the electrodes. The gap between electrodes is the distance that the ions have to travel in the electrolyte [77]. A smaller gap has the advantage of less resistance for ionic transportation. However, if the gap is too small, it would introduce electric sparks, posing an explosion hazard. Therefore, an optimal gap between electrodes has to be identified.

Another configuration factor, the electrolyte flow, determines the mass transport in the electrolyte. Circulating the electrolyte forces the species movement in the form of convection. At high current densities, electrochemical reactions are likely to be limited by the mass transfer of the electrolyte. High electrolyte flow conditions through rapid stirring or turbulence promoters eradicate the concentration difference and thus enhance the ions and mass transfer in the electrolyte.

## 6.2. Operating conditions

The overarching parameter is the operating cell voltage, which determines the energy consumption and electricity efficiency directly. A higher voltage at the same current to produce equivalent hydrogen means inefficiency.

The second important parameter is the operating current density, another parameter related to the energy efficiency directly. Conventional water electrolysers always run under the current density ranging from 1000 to 3000 A m$^{-2}$. The current density determines the rate of the hydrogen production. A higher current density means a greater electrochemical reactions rate. However, the rapid bubble formation resulted from increased gas production rate will increase the overpotential due to the greater bubble resistance. Consequently, the operating current density should be maintained within a certain range with compromises between gas production rates and energy efficiencies.

The operating temperature is another important parameter. Most of the conventional alkaline water electrolysers are designed to run at a temperature around 80–90 °C. As discussed in Section 3.1, the equilibrium voltage decreases as temperature increases. However, the higher the operating temperature, the

greater water loss due to evaporation and the more stringent demands for materials for the structural integrity [47]. Furthermore, the heat management and the material required for the diaphragm bring more engineering issues at higher operating temperatures.

Depending on the end use of the hydrogen, the pressure at which the electrolyser operates could be higher than atmospheric pressure. The elevated pressure cells operating at 3.5 MPa reduce the bubble sizes, minimising ohmic loss due to bubbles. Generally, the efficiency of pressured cells is not significantly superior to that of ambient pressure cells [78]. Pressurised operating environments increase the proportions of dissolved gas and require a more endurable diaphragm.

The type and concentration of the electrolyte are also important in the electrolysis due to the ionic transfer in the electrolyte. Good conductance of an electrolyte helps ionic transfer in the solution. As indicated in Section 5.2, the electrolyte concentration also plays an important role in determining the electrical resistance of the electrolyte. 25–30% potassium hydroxide is widely adopted in commercial electrolysers [79].

The stability of the electrode material is essential to the longevity of the electrolysers which are expected to serve for as long a time as possible to minimise the operating and maintenance costs from the economical point of view. The electrodes operate in very corrosive alkali environments, thus need to be resistant to the alkali attacks. Nobel metals have the alkali resistance and high electrochemical activities desired but are too expensive for widespread applications in water electrolysis [43]. Transition metals such as iron and copper possess good electrochemical activities but are less resistant to the alkali attacks. Nickel is the best electrode material for alkaline water electrolysis with good alkali resistance and electrochemical activity, while not being too expensive.

## 6.3. Water quality requirements

The purity of water is crucial for endured operations of electrolysers as impurities can accumulate in the electrolysers, deposit on the electrode surfaces and in the membrane, thus hampering the ions transfer and electrochemical reactions. The impurities in the electrolyte such as magnesium, calcium ions and chloride ions can also cause side reactions. Due to the alkaline environment in electrolysis cell, the concentrations of magnesium and calcium ions should be sufficiently low to avoid the blockage on the surface of electrode or diaphragm, hindering the mass and electron transfer [80]. The chloride ions in the alkaline solution are oxidised when the current density exceeds so-called hydroxyl ions limiting current [55], leading to the formation of chlorine at the anode surface, which is highly corrosive to the metal structures of the electrolysers.

The deposition of salts formed from the impurity metal ions is ruled by their own solubility product constant ($K_{sp}$) which is the limiting value for deposition to happen [52]. The constant is the chemical equilibrium between solid and dissolved states of a compound at saturation. When the product of the concentration value of each of these impurity metal ions and the power of its stoichiology number in the molecule reaches this limitation, the deposition will form. Table 3 lists those $K_{sp}$ of possible depositions with their ions to provide the criteria for choosing alkaline concentrations.

Take a solution with a pH of 14 under 25 °C for example, the concentration of hydroxyl ions is 1 mol/L and then the critical concentration of $Mg^{2+}$ is $1.8 \times 10^{-11}$ mol/L. $Mg(OH)_2$ deposition will form when the concentration of $Mg^{2+}$ ions exceeds this value.

**Table 3**
Solubility product constants of impurities at 25 °C.

| Ions/deposit | $K_{sp}$ (at 25 °C) |
|---|---|
| $Ca^{2+}/Ca(OH)_2$ | $5.5 \times 10^{-6}$ |
| $Mg^{2+}\ Mg(OH)_2$ | $1.8 \times 10^{-11}$ |
| $Ni^{2+}/Ni(OH)_2$ | $2.0 \times 10^{-15}$ |
| $Ag^+/AgCl$ | $1.6 \times 10^{-10}$ |
| $Zn^{2+}/Zn(OH)_2$ | $1.8 \times 10^{-14a}$ |

$^a$ Measured under 20 °C.

### 6.4. System considerations

The hydrogen production capacity of an electrolyser is an important parameter for judging the performance of an electrolyser. According to the need of energy or hydrogen, electrolysers of different scales are designed to meet the varying needs of the end users. It can be expressed in terms of hydrogen production rate in the unit of $N\,m^3\,h^{-1}$. Commercially, an electrolyser can vary from the several kW to several hundred MW in terms of power consumption [78]. Alternatively, embracing the volume of the electrolyser, the hydrogen production rate in the unit of $N\,m^3\,m^{-3}\,h^{-1}$ symbolises the mobility and capacity of the electrolyser.

As discussed in Section 3.2, the efficiency is an important parameter to compare the efficacy of different electrolyser technologies. The efficiency is a critical criterion either from energy or hydrogen production point of view. $\eta_{net\ efficiency}$ considers the efficacy of an electrolyser from the net energy point of view; an efficiency of around 50% for low temperature alkaline water electrolysis is considered to be good [81]. On the other hand, $\eta_{H_2yield}$ is useful when considering the hydrogen production at per volume electrolysis at unit time, for example, around $2.3\,m^3\,m^{-3}\,h^{-1}\,kWh^{-1}$ for a monopolar water electrolyser [78].

From the safety point of view, the wide range of the flammability limits of hydrogen and oxygen mixture demands careful design of the system configurations and the membrane. Leakage of the electrolyte is also a safety issue. Due to the corrosive nature of the electrolyte, the leakage is more likely to occur at the connections and the seals of the electrolyser. Bipolar cell configuration, which employs a more complex design, poses a higher risk of electrolyte leakage than the monopolar design.

The durability of the cell is also an important criterion for electrolysers. Materials for cell construction determine the cell lifespan. For alkaline electrolysis, these materials should be resistant to the high concentrations of alkaline electrolyte. Corrosion always happens more readily at the joints and connections, therefore the joint seal materials should also be stable under the operating environments.

## 7. Historical development of water electrolysis

This section reviews the development of the water electrolysis over the past two hundred years since the discovery of the water electrolysis. From the discovery of the phenomenon of electrolytic split of water into hydrogen and oxygen to the development of various versions of industrial technique to meet the hydrogen demands of various applications, the water electrolysis development has gone through several landmarks. Some historical events of water electrolysis are listed in the Table 4.

Those events in Table 4 promoted the development of this technology. Generally, we may classify the developments of water electrolysis into five stages

1. The discovery and recognition of water electrolysis phenomena (1800s–1920s).

**Table 4**
Historical events of water electrolysis.

| Year | Landmark event |
|---|---|
| 1800 | Nicholson and Carlisle discovered the electrolytical splitting of water [22] |
| 1920s | Several large 100 MW size plants were built worldwide [38] |
| 1948 | First pressurised electrolyser was built by Zdansky/Lonza [22] |
| 1966 | First solid polymer electrolyte system was built by General Electric Company [82] |
| 1970s | First solid oxide water electrolysis was developed [83] |

2. The technology became industrialised and mature for hydrogen production for industrial uses such as ammonia production and petroleum refining (1920s–1970s).
3. Systematic innovations were initiated to improve the net efficiency due to the fear of energy shortage and environmental considerations. The advancement in the space exploration drove the development of proton exchange membrane (PEM) water electrolysis, which is essentially the reverse of the PEM fuel cell operations, and military needs provoked the development of high pressure compact alkaline water electrolysis for submarine applications (1970s–present).
4. Rapidly evolving conceptual development to integrate water electrolysis with renewable energy technologies as a means for distributed energy production, storage and use as well hydrogen gas utilities, especially in remote communities (present).
5. Emergence of new water electrolysis concepts such as photovoltaic (PV) electrolysis that integrates the photoelectric effect and water electrolysis into one coherent operation, and steam electrolysis that employs a solid state electrolyte to effect the split of water molecules in steam (recent developments). These will be discussed in some detail in Section 8 on Recent innovations.

In the first stage, following the discovery of electricity, the phenomenon of water electrolysis was observed. Out of curiosity, the phenomenon was studied; the gases produced by electrolysis were finally identified to be hydrogen and oxygen [22], and gradually recognised for its potential applications. With the development of electrochemistry, the proportional relationship between the electrical energy consumption and the amount of gases produced became established through the Faraday's law of electrolysis. Finally the concept of water electrolysis was scientifically defined and acknowledged [52].

The second stage was the "golden" age for water electrolysis technology development. Most traditional designs were developed in this stage. Driven by the industrial need of hydrogen and oxygen, the knowledge established in the first stage was applied to the industrialisation of water electrolysis technologies. Stereotype of commercial water electrolysis developed at this stage included some important technology components that are still being used today [84].

One of the concepts still being applied in electrolyser is membrane. The function of membrane is to selectively allow the ions to pass through but not the gases. It realises the separation of the hydrogen and oxygen in the water electrolysers with some inhibition on the ionic transfer. It was demonstrated that the benefits of being able to separate the hydrogen and oxygen gases out weight the ohmic resistance brought about by the diaphragms. The first commercialised membrane was asbestos which was popular in the early stage. However, asbestos was found not very resistant to corrosion due to the strong alkaline environment at elevated temperatures. More recently, due to its seriously adverse health effect, asbestos was gradually replaced by other materials

[85]. Since the 1970s, the gas separation material has gradually shifted to polymers such as perfluorosulphonic acid, arylene ether and polytetrafluoroethylene [85,86].

Another significant development was the configurations of the electrolysis cells. As introduced before, they are monopolar and bipolar designs presented in the history. Typical conventional tank cells, with monopolar configuration, have the advantages of simplicity, reliability and flexibility. In contrast, filter press cells, with bipolar configuration, have the advantages of low ohmic loss and being more compact. High pressure electrolysers using bipolar configuration would be hard to achieve with the monopolar cells. The disadvantages of bipolar cells are their structural complexity and requirement of electrolyte circulation and gas electrolyte separators.

The electrode material selection is based on a dedicated balance amongst the desires for the corrosion resistance, high conductivity, high catalytic effect and low price [43]. Stainless steel is a cheap electrode material with low overpotential, however, steel could not resist high concentration alkaline solutions. Other materials such as lead and noble metals are either not resisted to the alkaline or too expensive to be used as bulk materials for the electrodes. Nickel has been identified to be a very active material with better corrosion resistance to the alkaline than other transition metals. It became popular in the water electrolysers during the electrolyser development. As compared in Table 1, nickel exhibits reasonable high hydrogen generation activity. Much research effort has been devoted to the understanding of the influence of physical property and the effects of the nickel-based alloys [87–89].

These developments stimulated the commercialisation of the electrolysis. The history of the commercial water electrolysis dates back to 1900, when water electrolyser technique was still in its infancy. Two decades later, large size plants, rated at 100 MW, were developed in Canada, primarily for the ammonia fertilisers [38].

Electrolyser manufacturers all over the world made a great effort to build their own energy systems to meet different needs. By late 1980, Aswan installed 144 electrolysers with a nominal rating of 162 MW and a hydrogen generation capacity of 32,400 $m^3\,h^{-1}$. Another highly modularised unit is the Brown Boveri electrolyser which can produce hydrogen at a rate of about 4–300 $m^3\,h^{-1}$. A number of electrolyser companies and their water electrolysis units are listed and compared in Table 5:

There are also some more companies not mentioned in this table. Stuart Cell (Canada) is the only monopolar tank-type cell manufacturer. Hamilton Sundstrand (USA), Proton Energy Systems (USA), Shinko Pantec (Japan) and Wellman-CJB (UK) are among the manufacturers of the latest PEM electrolysers.

The key driver for the development of the water electrolysis technology in the first half the 20th century was the need of hydrogen for the production of ammonia fertilisers which was also facilitated by the low cost of hydroelectricity. As the massive hydrocarbon energy was increasingly applied in the industry, the economical advantage of water electrolysis gradually faded as coal gasification and natural gas reforming became able to produce hydrogen in large scales at much lower costs. This resulted in the cease of the progress of the water electrolysis technology as a means for hydrogen production. However, the oil crisis in the 1970s provoked a renewed interest in water electrolysis worldwide and hydrogen was considered as the future energy carrier [17].

After the energy crisis in the 1970s, hydrogen as an energy carrier was considered a promising method to solve the energy security and sustainable energy supply problems, in the hydrogen economy ideology. Hydrogen production by water electrolysis received renewed interest and improving efficiency becomes a major goal. Some novel breakthroughs have been achieved at the cell system level with the emergence of pressurised electrolysers and PEM electrolyser [78].

Compact high pressure water electrolysers have been utilised to produce oxygen on board of nuclear powered submarines as part of the life-support system. An important feature of the design is the elimination of gaskets between cells which necessitates high precision machining of the cell frames. The deficiency of high pressure electrolyser is the characteristic pressure of the system up to 3.5 MPa, posing a great demand for safety [17].

For special energy need in the space area, a thin Nafion membrane was first applied by General Electric in 1966 [78]. The discovery of proton exchange membrane (PEM), realised the PEM water electrolysis, also named as solid polymer electrolysis (SPE). In an operation that reverses the PEM fuel cell, the PEM functions as the electrolyte to transfer the proton. Intensive studies have been carried out in order to reduce the cost of the membrane manufacturing. Subsequently, small-scale PEM water electrolysers were used for military and space applications in the early 1970s. However, the short durability of membrane makes PEM electrolysers too expensive for general applications [82].

PEM water electrolysis systems offer several advantages over traditional alkaline water electrolysis technologies including greater energy efficiency, higher production rates, and more compact design [20,90]. However, there are several disadvantages of the PEM electrolysis. PEM electrolysers have more special requirements on the components, including expensive polymer membranes and porous electrodes, and current collectors [30].

**Table 5**
Water electrolyser developers and cell operating conditions [47].

| Parameter | De Nora S.A.P | Norsk Hydro | Electrolyzer Corp. Ltd. | Teledyne Energy systems | General Electric |
|---|---|---|---|---|---|
| Cell type | B-FP | B-FP | M-T | B-FP | B-FP |
| Anode | Expanded Ni-plated Mild steel | Activated Ni-coated Steel | Ni-coated Steel | Ni screen | PTFE-bonded Noblemetal |
| Cathode | Activated Ni-plated Steel | Activated Ni-coated Steel | Steel | Ni screen | PTFE-bonded Noblemetal |
| Pressure (MPa) | Ambient | Ambient | Ambient | 0.2 | 0.4 |
| Temperature (°C) | 80 | 80 | 70 | 82 | 80 |
| Electrolyte | 29% KOH | 25% KOH | 28% KOH | 35% | Nafion |
| Current density (A m$^{-2}$) | 1500 | 1750 | 1340 | 2000 | 5000 |
| Cell voltage (V) | 1.85 | 1.75 | 1.9 | 1.9 | 1.7 |
| Current efficiency (%) | 98.5 | 98.5 | >99.9 | NR | NR |
| Oxygen purity (%) | 99.6 | 99.3–99.7 | 99.7 | >98.0 | >98.0 |
| Hydrogen purity (%) | 99.9 | 98.9–99.9 | 99.9 | 99.99 | >99.0 |

A comparison of typical alkaline and PEM electrolysers are summarised in Table 6.

## 8. Recent innovations

There have been a number of exciting new developments in the field of water electrolysis. This section discusses the recent innovations and research trends of the water electrolysis technology.

From the theoretical aspect, the water electrolysis has to reduce several resistances inherent in the process. Innovations have been made towards reducing the energy losses. These recent innovations and improvements are novel relative to the existing concepts of the water electrolysis but inevitably have their own limitations.

### 8.1. Photovoltaic (PV) electrolysis

The utilisation of solar energy as the source of electricity for water electrolysis was first reported by Fujishima and Honda [91]. A titanium dioxide electrode was applied to capture the energy of ultraviolet light. The captured energy, in the form of electricity, was applied to decompose water into hydrogen and oxygen directly as illustrated in Fig. 13. As renewable energy is receiving increasingly more interest, the PV electrolysis becomes another innovation of the water electrolysis for hydrogen production.

The PV electrolysis has two circuits in the system, as shown in Fig. 13, photovoltaic cell and electrolysis circuit. The key component in the PV electrolysis is the photo-electrodes which have to absorb energy from the sunshine and release electricity to split water through electrons. Most of the efforts have been devoted to developing semiconductor photo-electrically active materials.

The major deficiency of the PV electrolysis is the low energy conversion. Typical efficiency values of 2–6% restrict the large scale hydrogen production by the PV electrolysis [92]. Licht et al. reported a theoretical maximum net efficiency of 18.3% [93]. However, this figure was derived by assuming that all the electricity produced by the PV was converted to hydrogen. In other words, the Faraday efficiency was assumed to be 100%.

Practically, the applications of PV electrolysis on large scales are not optimistic at this stage of its development as compared to other existing and emergent technologies due to the low solar energy density, variations of sun radiation energy, low operation current density and the expensive and unstable electrode materials [94].

There are also research efforts aimed to combine the PV module and electrolyser together through the current control for the voltage regulation. By attaching a Co and Mo alloy and the Fe and Ni oxide electrodes for hydrogen and oxygen evolution, respectively, to a silicone PV solar cell, water electrolysis could be conducted simply by dipping the device in an electrolyte and irradiating it with ultraviolet light. This achieved a conversion efficiency of 2.5% from solar energy to hydrogen [95].



**Fig. 13.** A schematic diagram of semiconductor-based solid state photovoltaic electrolysis.

### 8.2. Steam electrolysis

Steam electrolysis or vapour electrolysis is performed using solid oxide electrolysis cell (SOEC) as shown in Fig. 14. This may be viewed in simple terms as the reverse operation of a solid oxide fuel cell. It is high temperature water electrolysis adopting the solid oxide as the electrolyte instead of liquid alkaline. It adapts a high temperature operating environment, around 820–1073 K, at which water splitting is thermodynamically favoured [96].

The stream passes through the cathode side of the solid electrolyte where hydrogen ions are reduced to hydrogen, releasing oxide ions in the process. The oxide ions then migrate through the electrolyte to the anode where they combine to form oxygen molecules, releasing an electron current following back to the power source [96,97].

The reactions on two electrodes are, respectively,

$$\text{Cathode}: \quad H_2O + 2e \rightarrow H_2 + O^{2-} \tag{R10}$$

$$\text{Anode}: \quad O^{2-} \rightarrow \frac{1}{2}O_2 + 2e \tag{R11}$$
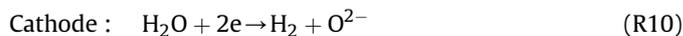
Hydrogen production via steam electrolysis may involve less electrical energy consumption than conventional low temperature water electrolysis, reflecting the improved thermodynamic and kinetic operating conditions at elevated temperatures. For an average current density of 7000 A m$^{-2}$ and an inlet steam temperature of 1023 K, the predicted electrical energy consumption of the stack is around 3 kWh per normal m$^3$ of hydrogen, which is significantly smaller than 4.5 kWh of low temperature alkaline water electrolysis cells commercially available today [98]. However, this result does not include the heating energy circulation and loss. Furthermore, construction materials, safety issues and strict temperature control have to be addressed as well.

### 8.3. Comparison of technologies

A comparison of different water electrolysis technologies is listed in Table 7. However, these data have different definitions of

**Table 6**
A comparison of the two types of commercialised electrolysers [78].

| Parameter | Monopolar alkaline electrolyser | PEM electrolyser/cell |
|---|---|---|
| Cell voltage | 1.85 | 2 V |
| Number of cells | N/A | 7–51 |
| Current density | 0.25 A cm$^{-2}$ | 1.075 A cm$^{-2}$ |
| Temperature | 70 °C | 65 °C (outlet) |
| Current | 10 kA | 1 kA (maximum) |
| Scale | 200 kW | N/A |
| Hydrogen production rate | 42 m$^3$ h$^{-1}$ | 0.42 m$^3$ h$^{-1}$ |
| Oxygen production rate | 21 m$^3$ h$^{-1}$ | 0.21 m$^3$ h$^{-1}$ |
| Hydrogen gas purity | H$_2$ > 99.5% | H$_2$ > 99.995% |
| Oxygen gas purity | O$_2$ > 99% | O$_2$ > 99% |
| Demineralized water conductivity | N/A | $\kappa < 0.25$ S cm$^{-1}$ |



**Fig. 14.** A schematic of SOEC planar stack unit for steam electrolysis.

**Table 7**
Comparison of different electrolyser technologies.

| Technology | Efficiency | Maturity | Reference |
|---|---|---|---|
| Alkaline electrolyser | 59–70%[a] | Commercial | [94] |
| PEM electrolyser | 65–82%[a] | Near term | [94] |
| Solid oxide electrolysis cells | 40–60%[b] | Mediate term | [94] |
| Photoelectrolysis | 2–12%[a] | Long term | [93] |

[a] The efficiency based on the hydrogen yield.
[b] The net efficiency.

efficiencies. For alkaline, PEM and photoelectrolysis electrolysers, the hydrogen yield efficiency is calculated based on the high heating value of hydrogen. The efficiency of the solid oxide electrolysis cells is the net efficiency, considering the thermal energy losses of the system.

The above comparison clearly illustrates that the alkaline water electrolysis is currently mature with reasonable efficiency relative to the other emergent water electrolysis technologies. The PEM electrolyser with highest performance in terms of efficiency still needs to overcome the difficulties mentioned in Section 7. SOEC and PV electrolysis are faced with more challenges due to its severely corrosive operating environment and engineering issues such as high operating temperature and scaling up requirements. Therefore, modifications to the alkaline electrolysis to achieve a better efficiency offer a more realistic solution for large scale hydrogen production in the near future.

## 9. Research trends

Despite the emergence of the new concepts of water electrolysis as discussed in the previous section, the low temperature alkaline water electrolysis still holds the promise for commercial applications and deserves further development. Intensive studies have been done in these areas to promote the development of water electrolysis [99]. The current research trends of alkaline water electrolysis are discussed from several aspects including electrodes, electrolytes, the ionic transport and bubble formation. These research efforts are not only significant to the water electrolyser but also fundamentals of the electrochemistry.

### 9.1. Electrodes

Metal electrodes are normally adopted in the gas evolving processes. As discussed in kinetics and the development of electrolyser sections earlier, the most widely used electrode material is nickel because of its stability and favourable activity. However, deactivation is a main problem of the electrode material even for nickel. The mechanism of the deactivation of the nickel electrodes is nickel the hydride phase formation at the surface of the nickel electrodes due to high hydrogen concentration. The iron coating prevents nickel hydride phase from forming and hence prevents deactivation of the electrode [87]. Dissolved vanadium species are also found to activate nickel cathodes during hydrogen evolution in the alkaline media [53]. Addition of iron to the manganese–molybdenum oxides enhanced the stability of electrodes. The iron addition also enhanced the oxygen evolution efficiency. The formation of the nickel triple oxides seems responsible for the

enhancement of both oxygen evolution efficiency and stability [100]. Therefore, electrocatalysts are the key to enhancing and stabilising the electrode activity.

Apart from material selection, electrode modifications in cell design are also important in water electrolysis. The electrode surfaces are commonly modified by slits and holes to facilitate the escape of gas bubbles. The holes must be appropriate to prevent the gas trapping. Typical diameters for electrode perforation in alkaline water electrolysis are 0.1 and 0.7 mm for hydrogen and oxygen, respectively [43]. Louvered, finned or slotted electrodes are also used to remove bubbles.

### 9.2. Electrocatalysts

To some extent, the electrode itself is a catalyst by affecting the activation energy of the electrochemical reaction. However, doping or coating more stable and active layer is always used in electrode design. Similar to catalysts, electrocatalysts facilitate charge transfer or chemical reaction, reducing the activation energy of the reaction. The obvious effect of an electrocatalyst is to reduce the overpotential of either or both of the two half reactions. The role of the electrocatalyst is effected by the electronic structure of the electrodes. In the hydrogen evolution reaction, Ni, Pd, Pt with $d^8s^2$, $d^{10}s^0$, and $d^9s^1$ electronic configurations, exhibiting minimum overvoltage values and Zn, Cd, Hg with $d^{10}s^2$ electronic configuration showing maximum values. The spillover theory in electrocatalysis by Bockris et al. enables the understanding of the interaction between substances [17].

Alloys, with different electronic distributions in the metal, are adopted to improve the activity of electrodes. For example, alloy of Mo and Pt was found to be a significant upgrade of the electrolytic efficiency in comparison with its individual components and conventional cathode materials [101]. More examples are listed in Table 8. The Tafel slope and exchange current density of the hydrogen evolution reaction in alkaline solutions at temperature near 70 °C are used to compare the activities of Ni and Ni-based alloy.

The doping material could be chosen from a wide range of metals. Noble metals are commonly used as electrocatalysts. Ruthenium dioxide ($RuO_2$), prepared by pyrolysis and calcinations, clearly shows the electrocatalytic activity for oxygen evolution reaction.[106]. An anode electrocatalyst with the formula $Ir_xRu_yTa_zO_2$ has been claimed to achieve overall voltage of 1.567 V at $1\ A\ cm^{-2}$ and 80 °C, equating to an energy consumption of $3.75\ kWh\ N\ m^{-3}\ H_2$ and an efficiency of 94% with the total noble metal loading less than $2.04\ mg\ cm^{-2}$ [90]. Non-noble metals also find their electrocatalytic activities. The Li doping increases the electrical conductivity of these materials. The key to better performance is that the roughness factor increases with Li percentage up to 3% of Li, favouring oxygen evolution [107].

The physical properties of electrode materials also influence the electrocatalytic activity. Larger BET surface area and porosity of the oxide catalyst powder are found by the small La addition by Singh et al. [108]. They observed a reduction in the charge transfer resistance for the oxygen evolution reaction on the electrode made of oxide powder.

**Table 8**
Tafel slopes of Ni alloys.

| Material and preparation method | Electrolyte | Temperature (°C) | Tafel slope (mV) | $i_0$ (A cm$^{-2}$) | $\eta_{250}$[a] (mV) |
|---|---|---|---|---|---|
| Ni (wire) [102] | 30% NaOH | 70 | 99 | $5.5 \times 10^{-5}$ | 362 |
| Ni$_{79}$Mo$_{20}$Cd [103] | 1 M NaOH | 70 | 125 | N/A | N/A |
| Ni$_{70}$Mo$_{29}$Si$_5$B$_5$ (amorphous) [104] | 30% KOH | 70 | 118 | $1.8 \times 10^{-6}$ | 489 |
| Ni$_{60}$Mo$_{40}$ mixture (ball-milled 20 h) [105] | 30% KOH | 70 | 50 | $1.7 \times 10^{-2}$ | 58 |

[a] Hydrogen evolution reaction overpotential under 2500 A m$^{-2}$.

**Table 9**
Oxygen overpotential of different electrode materials.

| Composition formula | Method | $T$ (°C) | Electrolyte | $C$ (mol dm$^{-3}$) | $j$ (A m$^{-2}$) | $\eta_{oxygen}$ (mV) | Ref. |
|---|---|---|---|---|---|---|---|
| Ni + Spinel type Co$_3$O$_4$ | Thermo-decomposition | 25 | KOH | 1 | 1000 | 235 ± 7 | [108] |
| Ni + La doped Co$_3$O$_4$ | Thermo-decomposition | 25 | KOH | 1 | 1000 | 224 ± 8 | [108] |
| MnOx modified Au | Electro-deposition | 25 | KOH | 0.5 | 100 | 300 | [112] |
| Li10% doped Co$_3$O$_4$ | Spray pyrolysis | RT[a] | KOH | 1 | 10 | 550 | [107] |
| Ni | N/A | 90 | KOH | 50 wt% | 1000 | 300 | [113] |
| La$_{0.5}$Sr$_{0.5}$CoO$_3$ | Spray-stiner | 90 | KOH | 50 wt% | 1000 | 250 | [113] |
| Ni$_{0.2}$Co$_{0.8}$LaO$_3$ | Plasma jet projection | 90 | KOH | 50 wt% | 1000 | 270 | [113] |

[a] Room temperature.

Nanostructure has also received much attention as it enlarges the material surface area and enables a unique electronic property. The increased active area of the nanostructured electrode reduces the operating current density of the electrolyser. A 25% reduction in overpotential and 20% reduction in energy consumption were achieved by the use of the Ru nano-rod cathode compared to the planar Ru cathode. The improvement was attributed to the increased active area of the nanostructured electrode which reduces the operating current density of the electrolyser [44]. Kamat [109] also proposed different nanostructures for improving the performance of photo-electrolysis facilitating the charge transfer, which has the potential to be applied as electrodes for water electrolysis.

The preparation methods of electrodes are an important factor in terms of effecting electrode surface properties such as roughness. Coatings are another common technique in electrode preparation. For example composite of Ni, Fe and Zn prepared from the electrodeposition showed good stability for up to 200 h under the current density of 1350 A cm$^{-2}$. This material showed good activity as well; in 28% KOH under 80 °C, its overpotential is about 100 mV which is significantly lower than that of mild steel (400 mV) [110]. A catalyst-coated membrane (CCM) with a five-layer structure was developed [111]. The five-layer CCM exhibits the highest performance and stability, attributed to the expansion of the triple-phase boundaries for electrochemical reactions and the improvement of contact and mass transfer resistance.

Tables 9 and 10 list several electrocatalysts which are found helpful to reduce the overpotential or stabilise the electrodes of the industrial water electrolysis.

To sum up, the physical modifications of electrodes help the removal of the gas from the electrodes. The electrode material influences the overpotential significantly. The electronic property and the surface property determine electrocatalytical performance of the coating or doping. Alloys, nanostructured materials, transition metals and noble metals could be used to improve the electrode activity.

### 9.3. Electrolyte and additives

Most commercial electrolysers have adopted alkali (potassium or sodium hydroxide) solutions as the electrolyte. Energy consumption during the electrolysis of water was significantly reduced by small quantities of activating compounds by the effect of ionic activators [121,122].

Ionic liquids (ILs) are organic compounds. At room temperature, they are liquids solely consisting of cations and anions, thus possessing reasonably good ionic conductivities and stability [123]. Imidazolium ILs were used as an electrolyte for hydrogen production through water electrolysis. The current densities higher than 200 A m$^{-2}$ and efficiencies greater than 94.5% are achieved using this ionic liquid in a conventional electrochemical cell with platinum electrodes at room temperature and atmospheric pressure. The catalytic activity of the electrode surface was not affected during the electrolysis mainly due to the chemical stability of the ILs [124]. However, the ILs normally have high viscosity and low water solubility which is not favoured for mass transport, resulting low achievable current densities and thus low hydrogen production rates. Therefore, more suitable ionic liquids with high conductivity and solubility are needed to facilitate electron transfer and water electrolysis, respectively.

Compared to the research on electrocatalysts, developmental effort on new electrolyte is relatively low. However, there is still a potential to improve the overall efficiency by using electrolyte additives to enhance ionic transfer by reducing the electrolyte resistance. On the other hand, the adoption of electrolyte additives could tune the affinity between electrolyte and electrodes and help to manage the bubble behaviour.

### 9.4. Bubble management

The bubble formation and its transportation are major causes of extra ohmic losses. Not only the dissolution of gas, but also the interface of gas between electrodes and electrolyte leads to resistances to water electrolysis.

The bubble behaviours are intensively studied [68,71,125] in the sense of electrochemistry, but no mechanisms or models have been applied to alkaline water electrolysis. Microgravity condition was used to study the bubble behaviours without the buoyancy effect. Water electrolysis under microgravity resulted in stable froth layer formation, and the accompanying ohmic resistance increased with the froth layer thickness. The contributions of electrode surface coverage by bubbles and electrolyte-phase bubble void fraction to

**Table 10**
Hydrogen overpotential of different electrode materials.

| Composition formula | Method | $T$ (°C) | Electrolyte | $C$ (mol dm$^{-3}$) | $j$ (A m$^{-2}$) | $\eta_{hydrogen}$ (mV) | Ref. |
|---|---|---|---|---|---|---|---|
| Ni–Fe–Mo–Zn | Co-deposition | 80 | KOH | 6 | 1350 | 83 | [114] |
| Ni–S–Co | Electro-deposition | 80 | NaOH | 28 wt% | 1500 | 70 | [115] |
| Ni50%–Zn | Electro-deposition | N/A | NaOH | 6.25 | 1000 | 168 | [116] |
| MnNi$_{3.6}$Co$_{0.75}$Mn$_{0.4}$Al$_{0.27}$ | Arc melting | 70 | KOH | 30 wt% | 1000 | 39 | [117] |
| Ti$_2$Ni | Arc melting | 70 | KOH | 30 wt% | 1000 | 16 | [118] |
| Ni50%Al | Melting | 25 | NaOH | 1 | 1000 | 114 | [119] |
| Ni75%Mo25% | Co-deposition | 80 | KOH | 6 | 3000 | 185 | [120] |
| Ni80%Fe18% | Co-deposition | 80 | KOH | 6 | 3000 | 270 | [120] |
| Ni73%W25% | Co-deposition | 80 | KOH | 6 | 3000 | 280 | [120] |
| Ni60%Zn40% | Co-deposition | 80 | KOH | 6 | 3000 | 225 | [120] |
| Ni90%Cr10% | Co-deposition | 80 | KOH | 6 | 3000 | 445 | [120] |

the ohmic drop were also studied [72]. Under territorial gravity, the bubble sizes are smaller. Therefore, reducing the residence time of bubble staying in the electrode is the key to minimising the bubble size and thus reducing the bubble resistance.

According to the theory of surface tension, a hydrophilic electrode prefers water rather than bubbles. It means the bubble sizes are not easy to grow. The mass transfer and ionic transfer between electrodes and electrolyte could be enhanced. Similarly, surfactant additive can be used to reduce the surface tension, which can minimise the bubble size or accelerate the departure of the bubbles and then achieve the same effect of hydrophilic materials. At the same time, these additives should be inert to the electrochemical reaction [126] and stable during the process.

Fluid mechanic means, by circulating the electrolyte solution to sweep the bubbles off the electrode surfaces can also be applied. To sweep the bubbles off the electrode surface, the velocity of the fluid should be high enough, which in turn will benefit the mass transfer of the electrolyte and eliminate the concentration difference. Therefore, mechanically forcing the bubble to depart from the electrode surface is an alternative way to eliminate the bubble formed on the electrode surface.

## 10. Summary

Alkaline water electrolysis combined with renewable energy can be integrated into the distributed energy system by producing hydrogen for end use and as an energy storage media. Compared to the other major methods for hydrogen production, alkaline water electrolysis is simple but currently less efficient. The challenges for widespread use of water electrolysis are also the durability and safety. These disadvantages require further research and development effort.

This paper has examined the fundamentals of the water electrolysis and compared the performance of various water electrolysis designs as well as introduced several emergent water electrolysis technologies.

Based on the thermodynamic and kinetic analyses of the alkaline water electrolysis, a number of resistances hindering the efficiency of the alkaline water electrolysis process have been identified. These include resistances due to bubbles, reaction activation energy, ionic transfer and electrical resistances in the circuit. The bubble resistance is suggested to be reduced by electrode modification and electrolyte additives. Reaction overpotential can be optimised by electrode material selection and preparation. In addition, transport-related resistances such as bubble resistance and electrolyte resistance can be reduced by improving mass transport such as bubble elimination by electrolyte circulation. By identifying the resistances causing extra energy losses, this study opens the opportunities to minimise the energy input especially at high current density.

Practical considerations of industrial electrochemical engineering and electrolyser development have led to the conclusion that the alkaline water electrolysis is still a better means for hydrogen production. Further R&D efforts to improve the efficiency are needed to widespread the application of the alkaline water electrolysis. These include developing electrocatalysts to significantly reduce electrochemical reaction resistance, electrolyte additives to facilitate the electron transfer and ionic transfer and to reduce electrode surface tension, electrode surface profile modifications and surface coatings, and more importantly, managing the gas bubble resistances.

## Acknowledgements

## References

[1] Barreto L, Makihira A, Riahi K. The hydrogen economy in the 21st century: a sustainable development scenario. Int J Hydrogen Energy 2003;28: 267–84.
[2] Mueller-Langer F, Tzimas E, Kaltschmitt M, Peteves S. Techno-economic assessment of hydrogen production processes for the hydrogen economy for the short and medium term. Int J Hydrogen Energy 2007;32:3797–810.
[3] Ramachandran R, Menon RK. An overview of industrial uses of hydrogen. Int J Hydrogen Energy 1998;23:593–8.
[4] Lattin WC, Utgikar VP. Transition to hydrogen economy in the United States: a 2006 status report. Int J Hydrogen Energy 2007;32:3230–7.
[5] Eliezer D, Eliaz N, Senkov ON, Froes FH. Positive effects of hydrogen in metals. Mater Sci Eng A 2000;280:220–4.
[6] Eliaz N, Eliezer D, Olson DL. Hydrogen-assisted processing of materials. Mater Sci Eng A 2000;289:41–53.
[7] Richards M, Shenoy A. H$_2$-MHR pre-conceptual design summary for hydrogen production. Nucl Eng Technol 2007;39:1–8.
[8] Turner JA. Sustainable hydrogen production. Science 2004;305:972–4.
[9] Rosen MA, Scott DS. Comparative efficiency assessments for a range of hydrogen production processes. Int J Hydrogen Energy 1998;23:653–9.
[10] Trommer D, Noembrini F, Fasciana A, Rodriguez D, Morales A, Romero M, et al. Hydrogen production by steam-gasification of petroleum coke using concentrated solar power – I. Thermodynamic and kinetic analyses. Int J Hydrogen Energy 2005;30:605–18.
[11] Momirlan M, Veziroglu TN. Current status of hydrogen energy. Renew Sust Energy Rev 2002;6:141–79.
[12] Sato S, Lin SY, Suzuki Y, Hatano H. Hydrogen production from heavy oil in the presence of calcium hydroxide. Fuel 2003;82:561–7.
[13] Stojic DL, Marceta MP, Sovilj SP, Miljanic SS. Hydrogen generation from water electrolysis – possibilities of energy saving. J Power Sources 2003;118:315–9.
[14] Tarasatti S. Water electrolysis: who first? J Electroanal Chem 1999;476:90–1.
[15] Dunn S. Hydrogen futures: toward a sustainable energy system. Int J Hydrogen Energy 2002;27:235–64.
[16] de Souza RF, Padilha JC, Goncalves RS, de Souza MO, Rault-Berthelot J. Electrochemical hydrogen production from water electrolysis using ionic liquid as electrolytes: towards the best device. J Power Sources 2007;164:792–8.
[17] Bockris JOM, Conway BE, Yeager E, White RE. Comprehensive treatise of electrochemistry. New York: Plenum Press; 1981.
[18] Turner JA. A realizable renewable energy future. Science 1999;285:687.
[19] Steinfeld A. Solar hydrogen production via a two-step water-splitting thermochemical cycle based on Zn/ZnO redox reactions. Int J Hydrogen Energy 2002;27:611–9.
[20] Grigoriev SA, Porembsky VI, Fateev VN. Pure hydrogen production by PEM electrolysis for hydrogen energy. Int J Hydrogen Energy 2006;31:171–5.
[21] Granovskii M, Dincer I, Rosen MA. Environmental and economic aspects of hydrogen production and utilization in fuel cell vehicles. J Power Sources 2006;157:411–21.
[22] Kreuter W, Hofmann H. Electrolysis: the important energy transformer in a world of sustainable energy. Int J Hydrogen Energy 1998;23:661–6.
[23] Bockris JO. The origin of ideas on a hydrogen economy and its solution to the decay of the environment. Int J Hydrogen Energy 2002;27:731–40.
[24] Bockris JOM, Veziroglu TN. Estimates of the price of hydrogen as a medium for wind and solar sources. Int J Hydrogen Energy 2007;32:1605–10.
[25] Isherwood W, Smith JR, Aceves SM, Berry G, Clark W, Johnson R, et al. Remote power systems with advanced storage technologies for Alaskan villages. Energy 2000;25:1005–20.
[26] Young DC, Mill GA, Wall R. Feasibility of renewable energy storage using hydrogen in remote communities in Bhutan. Int J Hydrogen Energy 2007;32:997–1009.
[27] Hanley N, Nevin C. Appraising renewable energy developments in remote communities: the case of the North Assynt Estate, Scotland. Energy Policy 1999;27:527–47.
[28] Hollmuller P, Joubert JM, Lachal B, Yvon K. Evaluation of a 5 kW(P) photovoltaic hydrogen production and storage installation for a residential home in Switzerland. Int J Hydrogen Energy 2000;25:97–109.
[29] Varkaraki E, Lymberopoulos N, Zachariou A. Hydrogen based emergency back-up system for telecommunication applications. J Power Sources 2003;118:14–22.
[30] Barbir F. PEM electrolysis for production of hydrogen from renewable energy sources. Solar Energy 2005;78:661–9.
[31] Agbossou K, Chahine R, Hamelin J, Laurencelle F, Anouar A, St-Arnaud JM, et al. Renewable energy systems based on hydrogen for remote applications. J Power Sources 2001;96:168–72.
[32] Degiorgis L, Santarelli M, Cali M. Hydrogen from renewable energy: a pilot plant for thermal production and mobility. J Power Sources 2007;171:237–46.
[33] Carter TJ, Cornish LA. Hydrogen in metals. Eng Fail Anal 2001;8:113–21.
[34] Suban M, Tusek J, Uran M. Use of hydrogen in welding engineering in former times and today. J Mater Process Technol 2001;119:193–8.
[35] Oi T, Sakaki Y. Optimum hydrogen generation capacity and current density of the PEM-type water electrolyzer operated only during the off-peak period of electricity demand. J Power Sources 2004;129:229–37.

[36] Kato T, Kubota M, Kobayashi N, Suzuoki Y. Effective utilization of by-product oxygen from electrolysis hydrogen production. Energy 2005;30:2580–95.

[37] Oldham KB, Myland JC. Fundamentals of electrochemical science. 1st ed. San Diego: Academic Press; 1993.

[38] Leroy RL. Industrial water electrolysis – present and future. Int J Hydrogen Energy 1983;8:401–17.

[39] Janjua MBI, Leroy RL. Electrocatalyst performance in industrial water electrolysers. Int J Hydrogen Energy 1985;10:11–9.

[40] Bird RB, Stewart WE, Lightfoot EN. Transport phenomena. 2nd ed. New York: John Wiley &Sons; 2007.

[41] Belmont C, Girault H. Coplanar interdigitated band electrodes for synthesis Part I: Ohmic loss evaluation. J Appl Electrochem 1994;24:475–80.

[42] Bard AJ, Faulkner LR. Electrochemical methods fundamentals and applications. 2nd ed. New York: John Wiley & Sons; 2001.

[43] Wendt H, Kreysa G. Electrochemical engineering. 1st ed. Berlin, Heidelberg: Springer-Verlag; 1999.

[44] Kim S, Koratkar N, Karabacak T, Lu T-M. Water electrolysis activated by Ru nanorod array electrodes. Appl Phys Lett 2006;88:2631061–3.

[45] Leroy RL, Bowen CT, Leroy DJ. The thermodynamics of aqueous water electrolysis. J Electrochem Soc 1980;127:1954–62.

[46] Rossmeisl J, Logadottir A, Norskov JK. Electrolysis of water on (oxidized) metal surfaces. Chem Phys 2005;319:178–84.

[47] Kinoshita K. Electrochemical oxygen technology. 1st ed. New York: John Wiley & Sons; 1992.

[48] Viswanath RP. A patent for generation of electrolytic hydrogen by a cost effective and cheaper route. Int J Hydrogen Energy 2004;29:1191–4.

[49] Bloom H, Futmann F. Electrochemistry: the past thirty and the next thirty years. 1st ed. New York: Plenum Press; 1977.

[50] Newman JS. Electrochemical systems. New Jersey: Prentice Hall; 1991.

[51] Pickett DJ. Electrochemical reactor design. 2nd ed. Amsterdam: Elsevier; 1979.

[52] Rieger PH. Electrochemistry. 1st ed. New Jersey: Prentice-Hall; 1987.

[53] Abouatallah RM, Kirk DW, Thorpe SJ, Graydon JW. Reactivation of nickel cathodes by dissolved vanadium species during hydrogen evolution in alkaline media. Electrochim Acta 2001;47:613–21.

[54] Trasatti S. Work function, electronegativity and electrochemical behaviour of metals: 2. Potentials of zero charge and electrochemical work functions. J Electroanal Chem 1971;33:351.

[55] Krstajic N, Popovic M, Grgur B, Vojnovic M, Sepa D. On the kinetics of the hydrogen evolution reaction on nickel in alkaline solution – Part II. Effect of temperature. J Electroanal Chem 2001;512:27–35.

[56] de Chialvo MRG, Chialvo AC. Hydrogen evolution reaction on a smooth iron electrode in alkaline solution at different temperatures. PCCP 2001;3:3180–4.

[57] Lee TS. Hydrogen overpotential on pure metals in alkaline solution. J Electrochem Soc 1971;118:1278.

[58] Correia AN, Machado SAS, Avaca LA. Studies of the hydrogen evolution reaction on smooth Co and electrodeposited Ni–Co ultramicroelectrodes. Electrochem Commun 1999;1:600–4.

[59] Choquette Y, Menard H, Brossard L. Electrocatalytic performance of composite coated electrode for alkaline water electrolysis. Int J Hydrogen Energy 1990;15:21–6.

[60] Miles MH, Huang YH, Srinivasan S. Oxygen-electrode reaction in alkaline-solutions on oxide electrodes prepared by thermal-decomposition method. J Electrochem Soc 1978;125:1931–4.

[61] Damjanov A, Dey A, Bockris JOM. Electrode kinetics of oxygen evolution and dissolution on Rh–Ir and Pt–Rh alloy electrodes. J Electrochem Soc 1966;113:739.

[62] Miles MH, Kissel G, Lu PWT, Srinivasan S. Effect of temperature on electrode kinetic parameters for hydrogen and oxygen evolution reactions on nickel electrodes in alkaline solutions. J Electrochem Soc 1976;123:332–6.

[63] Potvin E, Brossard L. Electrocatalytic activity of Ni–Fe anodes for alkaline water electrolysis. Mater Chem Phys 1992;31:311–8.

[64] Crow DR. Principles and applications of electrochemistry. 1st ed. London: Chapman and Hall; 1974.

[65] Hine F, Murakami K. Bubble effects on the solution IR drop in a vertical electrolyzer under free and force convection. J Electrochem Soc 1980;127:292–7.

[66] Macmullin RB, Muccini GA. Characteristics of porous beds and structures. AIChE J 1956;2:393–403.

[67] Dyer CK. Improved nickel anodes for industrial water electrolyzers. J Electrochem Soc 1985;132:64–7.

[68] Jones SF, Evans GM, Galvin KP. Bubble nucleation from gas cavities – a review. Adv Colloid Interf 1999;80:27–50.

[69] Defay R, Prigogine I. Surface tension and adsorption. 1st ed. London: Longmans; 1966.

[70] Adam NK. The physics and chemistry of surfaces. 1968.

[71] Kiuchi D, Matsushima H, Fukunaka Y, Kuribayashi K. Ohmic resistance measurement of bubble froth layer in water electrolysis under microgravity. J Electrochem Soc 2006;153:E138–43.

[72] Matsushima H, Nishida T, Konishi Y, Fukunaka Y, Ito Y, Kuribayashi K. Water electrolysis under microgravity – Part 1. Experimental technique. Electrochim Acta 2003;48:4119–25.

[73] Vogt H, Balzer RJ. The bubble coverage of gas-evolving electrodes in stagnant electrolytes. Electrochim Acta 2005;50:2073–9.

[74] Hine F, Yasuda M, Nakamura R, Noda T. Hydrodynamic studies of bubble effects on Ir-drops in a vertical rectangular cell. J Electrochem Soc 1975;122:1185–90.

[75] Dejonge RM, Barendrecht E, Janssen LJJ, Vanstralen SJD. Gas bubble behavior and electrolyte resistance during water electrolysis. Int J Hydrogen Energy 1982;7:883–94.

[76] Boissonneau P, Byrne P. An experimental investigation of bubble-induced free convection in a small electrochemical cell. J Appl Electrochem 2000;30:767–75.

[77] Nunes SP, Peinemann K-V. Membrane technology. 2nd ed. Weinheim: Wiley-VCH Verlag GmbH & KGaA; 2007.

[78] Pletcher D, Walsh FC. Industrial electrochemistry. 2nd ed. London: Blackie Academic & Professional; 1990.

[79] Gutmann F, Murphy OJ. Modern aspects of electrochemistry. New York: Plenum Press; 1983.

[80] Millet P, Andolfatto F, Durand R. Design and performance of a solid polymer electrolyte water electrolyzer. Int J Hydrogen Energy 1996;21:87–93.

[81] Council NR, Engineering NAo. The hydrogen economy; 2005.

[82] Lu PWT. Advances in water electrolysis technology with emphasis on use of the solid polymer electrolyte. J Appl Electrochem 1979;9:269.

[83] Spacil HS, Tedmon CS. Electrochemical Dissociation of water vapor in solid oxide electrolyte cells. I. Thermodynamics and cell characteristics. J Electrochem Soc 1969;116:1618.

[84] Bowen CT, Davis HJ, Henshaw BF, Lachance R, Leroy RL, Renaud R. Developments in advanced alkaline water electrolysis. Int J Hydrogen Energy 1984;9:59–66.

[85] Rosa VM, Santos MBF, Dasilva EP. New materials for water electrolysis diaphragms. Int J Hydrogen Energy 1995;20:697–700.

[86] Hickner MA, Ghassemi H, Kim YS, Einsla BR, McGrath JE. Alternative polymer systems for proton exchange membranes (PEMs). Chem Rev 2004;104:4587–612.

[87] Mauer AE, Kirk DW, Thorpe SJ. The role of iron in the prevention of nickel electrode deactivation in alkaline electrolysis. Electrochim Acta 2007;52:3505–9.

[88] Bocca C, Barbucci A, Cerisola G. The influence of surface finishing on the electrocatalytic properties of nickel for the oxygen evolution reaction (OER) in alkaline solution. Int J Hydrogen Energy 1998;23:247–52.

[89] Soares DM, Teschke O, Torriani I. Hydride effect on the kinetics of the hydrogen evolution reaction on nickel cathodes in alkaline media. J Electrochem Soc 1992;139:98–105.

[90] Marshall A, Borresen B, Hagen G, Tsypkin M, Tunold R. Hydrogen production by advanced proton exchange membrane (PEM) water electrolysers – reduced energy consumption by improved electrocatalysis. Energy 2007;32:431–6.

[91] Fujishima A, Honda K. Electrochemical photolysis of water at a semiconductor electrode. Nature 1972;238:37.

[92] Gibson TL, Kelly NA. Optimization of solar powered hydrogen production using photovoltaic electrolysis devices. Int J Hydrogen Energy 2008;33:5931–40.

[93] Licht S, Wang B, Mukerji S, Soga T, Umeno M, Tributsch H. Over 18% solar energy conversion to generation of hydrogen fuel; theory and experiment for efficient solar water splitting. Int J Hydrogen Energy 2001;26:653–9.

[94] Holladay JD, Hu J, King DL, Wang Y. An overview of hydrogen production technologies. Catal Today 2009;130:244–60.

[95] Yamada Y, Matsuki N, Ohmori T, Mametsuka H, Kondo M, Matsuda A, et al. One chip photovoltaic water electrolysis device. Int J Hydrogen Energy 2003;28:1167–9.

[96] Udagawa J, Aguiar P, Brandon NP. Hydrogen production through steam electrolysis: control strategies for a cathode-supported intermediate temperature solid oxide electrolysis cell. J Power Sources 2008;180:354–64.

[97] Brisse A, Schefold J, Zahid M. High temperature water electrolysis in solid oxide cells. Int J Hydrogen Energy 2008;33:5375–82.

[98] Udagawa J, Aguiar P, Brandon NP. Hydrogen production through steam electrolysis: model-based steady state performance of a cathode-supported intermediate temperature solid oxide electrolysis cell. J Power Sources 2007;166:127–36.

[99] Pettersson J, Ramsey B, Harrison D. A review of the latest developments in electrodes for unitised regenerative polymer electrolyte fuel cells. J Power Sources 2006;157:28–34.

[100] Abdel Ghany NA, Kumagai N, Meguro S, Asami K, Hashimoto K. Oxygen evolution anodes composed of anodically deposited Mn–Mo–Fe oxides for seawater electrolysis. Electrochim Acta 2002;48:21–8.

[101] Stojic DL, Grozdic TD, Marceta Kaninski MP, Maksic AD, Simic ND. Intermetallics as advanced cathode materials in hydrogen production via electrolysis. Int J Hydrogen Energy 2006;31:841–6.

[102] Huot JY, Brossard L. Time-dependence of the hydrogen discharge at 70-Degrees-C on nickel cathodes. Int J Hydrogen Energy 1987;12:821–30.

[103] Conway BE, Bai L. H$_2$ evolution kinetics at high activity Ni–Mo–Cd electro-coated cathodes and its relation to potential dependence of sorption of H. Int J Hydrogen Energy 1986;11:533–40.

[104] Huor JY, Trudeau M, Brossard L, Schulz R. Hydrogen evolution on some Ni-base amorphous alloys in alkaline solution. Int J Hydrogen Energy 1989;14:319–22.

[105] Huot JY, Trudeau ML, Schulz R. Low hydrogen overpotential nanocrystalline Ni–Mo cathodes for alkaline water electrolysis. J Electrochem Soc 1991;138:1316–21.

[106] Ma H, Liu C, Liao J, Su Y, Xue X, Xing W. Study of ruthenium oxide catalyst for electrocatalytic performance in oxygen evolution. J Mol Catal A: Chem 2006;247:7–13.

[107] Hamdani M, Pereira MIS, Douch J, Addi AA, Berghoute Y, Mendonca MH. Physicochemical and electrocatalytic properties of Li–Co$_3$O$_4$ anodes prepared by chemical spray pyrolysis for application in alkaline water electrolysis. Electrochim Acta 2004;49:1555–63.

[108] Singh RN, Mishra D, Anindita, Sinha ASK, Singh A. Novel electrocatalysts for generating oxygen from alkaline water electrolysis. Electrochem Commun 2007;9:1369–73.

[109] Kamat PV. Meeting the clean energy demand: nanostructure architectures for solar energy conversion. J Phys Chem C 2007;111:2834–60.

[110] Giz MJ, Bento SC, Gonzalez ER. NiFeZn codeposit as a cathode material for the production of hydrogen by water electrolysis. Int J Hydrogen Energy 2000;25:621–6.

[111] Song S, Zhang H, Liu B, Zhao P, Zhang Y, Yi B. An improved catalyst-coated membrane structure for PEM water electrolyzer. Electrochem Solid-State Lett 2007;10:B122–5.

[112] El-Deab MS, Awad MI, Mohammad AM, Ohsaka T. Enhanced water electrolysis: electrocatalytic generation of oxygen gas at manganese oxide nanorods modified electrodes. Electrochem Commun 2007;9:2082–7.

[113] Wendt H, Hofmann H, Plzak V. Materials research and development of electrocatalysts for alkaline water electrolysis. Mater Chem Phys 1989;22:27–49.

[114] Crnkovic FC, Machado SAS, Avaca LA. Electrochemical and morphological studies of electrodeposited Ni–Fe–Mo–Zn alloys tailored for water electrolysis. Int J Hydrogen Energy 2004;29:249–54.

[115] Han Q, Liu K, Chen J, Wei X. Hydrogen evolution reaction on amorphous Ni–S–Co alloy in alkaline medium. Int J Hydrogen Energy 2003;28:1345–52.

[116] Sheela G, Pushpavanam M, Pushpavanam S. Zinc–nickel alloy electrodeposits for water electrolysis. Int J Hydrogen Energy 2002;27:627–33.

[117] Hu W. Electrocatalytic properties of new electrocatalysts for hydrogen evolution in alkaline water electrolysis. Int J Hydrogen Energy 2000;25:111–8.

[118] Hu W, Lee J-Y. Electrocatalytic properties of Ti$_2$Ni/Ni–Mo composite electrodes for hydrogen evolution reaction. Int J Hydrogen Energy 1998;23:253–7.

[119] Los P, Rami A, Lasia A. Hydrogen evolution reaction on Ni–Al electrodes. J Appl Electrochem 1993;23:135–40.

[120] Raj IA. Nickel-based, binary-composite electrocatalysts for the cathodes in the energy-efficient industrial-production of hydrogen from alkaline-water electrolytic cells. J Mater Sci 1993;28:4375–82.

[121] Stojic DL, Grozdic TD, Marceta Kaninski MP, Stanic V. Electrocatalytic effects of Mo–Pt intermetallics singly and with ionic activators. Hydrogen production via electrolysis. Int J Hydrogen Energy 2007;32:2314–9.

[122] Marceta Kaninski MP, Maksic AD, Stojic DL, Miljanic SS. Ionic activators in the electrolytic production of hydrogen – cost reduction-analysis of the cathode. J Power Sources 2004;131:107–11.

[123] Endres F, El Abedin SZ. Air and water stable ionic liquids in physical chemistry. PCCP 2006;8:2101–16.

[124] de Souza RF, Padilha JC, Goncalves RS, Rault-Berthelot JL. Dialkylimidazolium ionic liquids as electrolytes for hydrogen production from water electrolysis. Electrochem Commun 2006;8:211.

[125] Vogt H. The problem of the departure diameter of bubbles at gas evolving electrodes. Electrochim Acta 1989;34:1429–32.

[126] Wei ZD, Ji MB, Chen SG, Liu Y, Sun CX, Yin GZ, et al. Water electrolysis on carbon electrodes enhanced by surfactant. Electrochim Acta 2007;52:3323–9.